NASA Technical Memorandum 89011

DESIGN AND FABRICATION OF LARGE SUCTION PANELS WITH PERFORATED SURFACES FOR LAMINAR FLOW CONTROL TESTING IN A TRANSONIC WIND TUNNEL

Dal V. Maddalon and
William A. Poppen, Jr.

AUGUST 1986

National Aeronautics and
Space Administration

Langley Research Center
Hampton, Virginia 23665

DESIGN AND FABRICATION OF LARGE SUCTION PANELS WITH PERFORATED SURFACES FOR LAMINAR FLOW CONTROL TESTING IN A TRANSONIC WIND TUNNEL

D. V. Maddalon and W. A. Poppen, Jr.
National Aeronautics and Space Administration
Langley Research Center
Hampton, Virginia

ABSTRACT

Considerable progress has been made in the development of structural panels with perforated suction surface material for laminar flow control application. Electron-beam perforated titanium skin was used as the suction surface. Critical issues related to suction panel manufacturing were identified and largely resolved. Techniques used could be adapted to modern aircraft production lines for laminar flow control wings. The final product included fabrication of a 7 foot chord by 7 foot span perforated laminar flow control wind tunnel model. This report includes details on the wind tunnel model panel instrumentation and other features required for testing in a transonic pressure tunnel.

SYMBOLS

c	Chord Length
C_l	Lift Coefficient
C_p	Pressure Coefficient
C_q	Suction Coefficient
D	Nozzle Diameter
DAC	Douglas Aircraft Company
EBP	Electron Beam Perforated
ID	Inner Diameter
L	Nozzle Length
LEFT	Leading Edge Flight Test
LFC	Laminar Flow Control
M	Mach Number
N	Disturbance Amplification Factor (e^N)
OD	Outer Diameter
P_d	Duct Pressure
P_f	Flute Pressure
P_s	Surface Pressure
R	Reynolds Number
x	Streamwise
y	Spanwise
W_{MD}	Wave Maximum Depth
W_A	Wave Average Depth

INTRODUCTION

Attainment of laminar flow on aircraft wings has significant potential for reducing aircraft drag and increasing fuel efficiency. One method used to maintain large chordwise extents of laminar flow is to suck a small part of the boundary layer through the wing skin. This method, called Laminar Flow Control (LFC), can stabilize the boundary layer to small disturbances and delay transition to turbulence. The basic theory is well established and has been verified in wind-tunnel testing and demonstrated in flight tests. References 1-4 list important works to 1982 on suction through narrow multiple slots, porous materials, and small perforations.

Continuous suction through a porous surface is an effective means of delaying boundary layer transition. Experimental verification of continuous suction effectiveness was reported in Reference 5 but was never applied to operational aircraft because of a lack of suitable porous materials for flight application. An approximation to continuous suction that appeared feasible was the use of narrow multiple spanwise suction slots. Early development efforts focused on this approach and eventually led to various flight tests, the most notable of which was the X-21 flight research program (Refs. 6-9). Technical feasibility was demonstrated, but operational practicality in a realistic environment remained to be accomplished. Another approximation to continuous suction through a porous surface is suction through small perforations (Ref. 10). Until recently, however, perforation of airplane materials with the small hole sizes required was beyond practical production manufacturing capabilities.

Important recent efforts to develop suitable porous and perforated surfaces are reported in References 11 - 14. These studies included, for example, woven materials, chemical etching techniques, and electron beam drilling. The latter offers great promise for cost-effective manufacture of practical and aerodynamically suitable perforated surfaces. The process was developed by Steigerwald Strahltechnic GMBH of West Germany and has been refined by the Pratt & Whitney Aircraft Company.

The main objective of the present work was to design and fabricate relatively large suction surface panels with aerodynamically satisfactory surface perforations, and with surface contour and smoothness characteristics necessary for a large scale laminar flow control wind tunnel test. Requirements of commercial transport production lines were carefully considered in panel development. Much could be learned about the practicality of such panels for aircraft applications, since panel size is representative of what could be used on a commercial transport wing. Tests of the perforated panels in a transonic wind tunnel could demonstrate aerodynamic suitability at conditions near full scale Reynolds number and flight Mach number. At these conditions, questions exist regarding perforated surface smoothness, contour waviness, and basic aerodynamic effectiveness with suction (Ref. 15). Results of recent tests on perforated surface aerodynamics at lower than flight length Reynolds numbers and Mach numbers are reported in References 12, 16,

17 and 18. Other recent laminar flow studies can be found in References 19 - 28.

To meet these objectives, three electron beam perforated (EBP) titanium suction panels were designed, developed and manufactured for the upper surface of a Langley 8 foot Transonic Pressure Tunnel LFC model previously tested with multiple suction slots. The suction panels represent one of the largest perforated LFC structures ever built with a chord as large as a small general aviation aircraft wing. A sketch of the model in the tunnel is given in Figure 1. The tunnel wall is faired with a liner to produce an effective infinite swept-wing flow over the model (Ref. 29). Figure 2 is the airfoil cross-section. The model has a 7.07 foot chord, 23 degrees sweep, thickness ratio of 13 percent, design chord Reynolds number of 20 million, and design lift coefficient of 0.551 at 0.755 Mach number. A flap extends over the aft 10.9 percent chord for use in pressure distribution control. Three panels which form the upper surface (Fig. 3) were built to the same contour used for the earlier tests on the slotted suction panels (Ref. 30, 31). The panels have a sandwich construction with the titanium skin bonded to a fiberglass corrugated core (forming flutes for subsurface airflow transfer) and a fiberglass and graphite inner face sheet. Impervious bond areas divide the panel surface such that suction through perforated strips occurs at the surface. Metering holes located in the bottom of the suction flutes transfer flow to aluminum ducts from which flow exits the tunnel. Ducts are attached to a wingbox support mounted to the tunnel walls.

This paper describes efforts made in the design and fabrication of the three upper suction panels. Also included is a description of the instrumentation and other model features required for the wind tunnel tests. The three suction panels and supporting ducts were fabricated by Douglas Aircraft Company (DAC) under NASA contract. NASA Langley instrumented the model and built supporting hardware.

DESIGN

The airfoil design pressure distribution (Ref. 30) incorporates the latest in supercritical technology and has a drag divergence Mach number comparable to modern turbulent airfoils. A significant region of supercritical flow exists on the upper surface. Features of the airfoil design point ($M = 0.755$, $C_l = 0.551$, $R = 20$ million) upper surface static pressure distribution include a short, steep favorable gradient near the leading edge caused by the small nose radius and a slightly adverse gradient over the majority of the chord with the aft region exhibiting a Stratford-type pressure recovery. Figure 4 illustrates where boundary layer crossflow and Tollmein-Schlichting disturbances are important. Streamwise crossflow vortices caused by wing sweep exist near the leading edge and aft chord region. Near mid-chord, Tollmein-Schlichting wave growth predominates. Figure 4 shows how suction applied to the boundary layer can control disturbance amplification such that transition is delayed. Near the leading edge, suction is

particularly advantageous in minimizing total suction required (Ref. 16, 20).

Although design Reynolds number for the perforated panels was 20 million, the design allows tests at Reynolds numbers as low as 8 million and as high as 40 million. The design suction distribution chosen by DAC for each Reynolds number is given in Figure 5. The MARIA boundary layer stability code (Ref. 21) was used for design.

Due to chordwise pressure gradient, the possibility exists that flow entering one flute may flow out of the same flute at a different chordwise location of lower surface pressure, or may flow out of a neighboring flute (when adjacent flutes are plumbed together) if the surface pressure drop is not sufficient (Fig. 6). This situation, which might cause transition, is most likely to occur in the leading and trailing edge regions where the chordwise pressure gradient is the greatest. This possibility was taken into account in the model design. Flute height, number of flutes per suction duct, nozzle size and location, metering hole size and spacing, and design suction distribution were chosen to insure that the pressure drop is as great as possible while keeping the basic design simple and minimizing fabrication cost. The flutes have been designed for a particular suction rate which varies with location. Mass flow rate, pressure, and pressure drop versus flute location is given in Table 1 for the design conditions. The duct number versus flute number and location is found in Table 2. To better control outflow due to chordwise pressure gradient and permit a finer suction distribution, the leading and trailing edge regions have fewer flutes per duct than does the mid-chord region.

Although the model and wind tunnel liner were designed to achieve an effective infinite swept wing flow with no spanwise flow gradients, spanwise pressure gradients may exist due to design imperfections. At some point along the span, surface pressure might become lower than flute pressure and flow entering at one point along the span might flow out into the boundary layer. Spanwise baffles (also see "Baffle" section) have been placed in the flutes to retard flow movement within the flute from one spanwise location to another.

Special development efforts were made to produce panels that meet LFC waviness criteria. Test panels (1 ft. by 1 ft.) were built with a maximum wave depth over flutes as small as 0.0004 in. and an average wave depth as small as 0.0003 in. Difficulties encountered in scaling up panel size combined with time and money constraints to prevent achievement of the same level of waviness on the much larger final panels. The small scale results, however, do indicate what might be possible for large scale panels with further effort. Contour dimensions were checked by both detailed measurements on a Cordax machine and by measuring deviation from streamwise and chordwise templates. For the final panels, the worst waviness occurred in the aft panel which had some short waves as great as $\pm$0.002 in. (which approximates X-21 waviness criteria). This panel was hand polished to improve surface finish.

The suction pattern in the aft panel turbulent region near the tunnel walls was set by filling in with lacquer some EBP holes such that a "ramped" suction distribution was obtained (Fig. 7). Maximum suction required is at the model edge. Table 3 presents the model area and location filled for each turbulent flute.

FABRICATION

Model suction panels and ducts were built by DAC using practical aerospace manufacturing techniques to ensure that fabrication methods would be compatible with industry work practices and assembly line techniques. A discussion of techniques employed during a similar fabrication can be found in References 12 and 14. To better suit the conduct of the wind tunnel tests, Langley made some alterations to the basic construction.

Leading Edge - The sharp nose radius was cold-rolled from titanium sheet. Leading edge design is shown in Figure 8. Hysol epoxy resin was fit-poured in the space between the suction panel and the aluminum duct to provide leading edge support. The leading edge joint between the upper forward suction panel and the forward lower panel was handworked to a very smooth fit.

Skin - The Pratt & Whitney electron beam perforation drilling process (Fig. 9) was used with 6AL-4V titanium skin 0.025 in. thick. With this thickness, a pore diameter of approximately 0.0025 in. is presently about the minimum hole diameter possible. Thickness is adequate to provide resistance to impact damage from rain, hail or accident in actual aircraft application (Ref. 12). Hole spacing is 0.025 in., yielding an open area porosity ratio of 0.8 percent. Drilling speeds for the Steigerwald process are shown in Figure 10. For the selected hole diameter and depth, about 1000 holes can be drilled per second. A natural result of the drilling process is a slag-free tapered hole with inner surface diameter about twice that of the outer diameter (Fig. 9). This provides protection from hole clogging if small debris is pulled through the skin. Perforated titanium sheets currently available are limited to 17 in. by 54 in. Since the required perforated titanium surface area was approximately 7000 sq. in., the smaller sheets were welded together (using Tungsten Inert Gas techniques) to form the panel skin. This technique produced a weld bead approximately 0.1 in. wide. An electron beam welding technique was tested which produced a smaller weld bead but was also more expensive. Both techniques cause some distortion of the titanium skin due to high local temperature. To correct joint distortion, "oil canning", sheets were heated to approximately 1200 deg. F. in an inert gas environment. At this temperature, titanium sheet becomes plastic and sags against a flat mold where it is held at temperature and pressure. The welded sheet is then roll-formed at room temperature to contour. In a production situation, the titanium might be hot-formed to contour while the weld distortions are removed (Ref. 14).

The titanium surface is alkaline etched, anodized with phosphoric acid, primed, and baked to improve bonding strength

between surface and flute structure. The bond must be made soon after priming to obtain best results from the low-flow AF-31 adhesive. Tests show that the preparation process does not significantly affect skin porosity.

Some variation in surface porosity, however, does occur. As a consequence, a technique was developed at Langley to permanently record the final porosity pattern of each panel (Fig. 11). Photographic film sheets (approximately the size of the LFC panels) are exposed in a dark room by passing a light through each flute. The film clearly shows blocked holes, flute locations, skin instrumentation holes, and titanium weld seam locations. This technique provided a permanent record of surface porosity for later correlation with actual LFC data. Resolution is so fine that both clear and blocked 0.0025 in. diameter holes can be seen. Hole blockage is caused by adhesive flow, manufacturing defects, seams, and flute supports. Generally about 10-15 percent of the holes were blocked due to defects in the electron beam drilling process and about 5 percent more blocked due to adhesive flow from skin bonding. Further refinement of the technique should reduce the amount of blocked holes. Brief attempts were made to clean the 0.0025 in. blocked holes mechanically using very fine drill rods but this was abandoned as it became evident that prohibitive costs would result because of the tiny hole diameter and fragile nature of the tool involved. Instead, resin-clogged EBP holes were cleaned using a 0.005 in. diameter, 50,000 psi water jet.

Obviously, for proper operation of the surface suction system, the model surface must be kept clean. The effect of steam cleaning an EBP surface is shown in Figure 12 which illustrates that such cleaning can restore original porosity.

Flutes - A steel female master tool was used to form the surface contour. Silicone mandrels (Fig. 13) were laid up on the master tool to form the flute fiberglass structure (Fig. 14). Figure 15 shows a typical flute-skin layup. Flutes alternate between suction (active) and non-suction (inactive) areas over the entire model providing a very simple laminar flow control ducting system. On the upper surface, there are 74 active flutes. The nominal chordwise suction length of the active flutes is 0.66 in., and the chordwise length of the bonded region (non-suction) is a nominal 0.30 in. The bond between the fiberglass flutes and titanium skin consists of AF-31 adhesive (3-M), fiberglass and graphite (Fig. 15). Flutes are composed of three layers of carbon fiber cloth plies (Ref. 14). The layering where the skin and flute meet balances the varying thermal coefficient of expansion between the dissimilar structural materials of fiberglass and titanium, and eliminates buildup of internal stresses which tend to cause panel bowing. Graphite used in layering helps balance thermal expansion coefficients which might otherwise result in surface waves. Bonding of skin to flute is accomplished on the master tool with the entire assembly cured in an autoclave (Fig. 16,17). No tool marks were transferred to the titanium skin, but a few marks were left due to wrinkles in the plastic which enclosed the skin-flute assembly during cure. These slight imperfections were later hand-polished, producing a smooth,

blemish-free panel surface. A completed panel is shown in Figure 18.

A flute spanwise bowing problem was solved by inserting a strip of graphite on the backside of the fiberglass substructure under each suction flute over the approximate seven-foot span. Typical compression, tension, and lap-shear strengths of panel structure can be found in Reference 14.

To seal the fiberglass flute wall, flutes were coated with a liquid epoxy prior to bonding. After bonding, a check for flute to flute leakage was made. Some flutes leaked, so epoxy was applied to the corners between the fiberglass and titanium (Figure 15). All flutes eventually passed the leakage criteria of a 30 second minimum allowable time for a pressure change from 10 in. Hg to 5 in. Hg (vacuum). This leak-rate corresponds to a mass flow less than 1 percent of the design test condition mass flow rate.

A tape manufactured by Airtech International Inc. was used to seal the perforated surface while making final leak-check measurements. This high temperature tape (Flashbreaker 2) is three mils thick, of polyester film (2 mil) and cured silicon adhesive (1 mil), and will not leave residue on the model surface.

Metering Holes - Metering holes (Fig. 19) to move flow from the flutes to the ducts are drilled through thin aluminum squares bonded to the backside of the active flutes (Figs. 20, 21). The metal squares allow a "clean" drilled circular hole as opposed to the irregular holes which resulted from drilling directly through the graphite and fiberglass. Hole size and spacing is used as a flow metering device for each flute. The metering hole system is designed to function for skin perforations of 0.0025 in. to 0.003 in. diameter. Metering hole size and number per flute partition versus flute location is given in Table 2. Metering hole size is critical to baffle effectiveness.

Baffles - If a spanwise pressure gradient exists, outflow of air may occur at a spanwise location corresponding to low external surface pressure. Outflow may be prevented by decreasing internal flute pressure to a value lower than the minimum external pressure although this results in excessive suction at all other spanwise locations. An effective method of minimizing outflow is to separate the spanwise flute into various compartments with baffles (Fig. 22). Baffles are trapezoidal in shape, conform to the flute inside contour, and are nominally spaced spanwise every 2.3 in. for the first 57 (Fig. 23) active flutes, and every 13.8 in. for active flutes 58-61. No baffles were needed in active flutes 62-74 due to the large amount of suction applied on the aft panel. Baffle spacing was determined assuming a constant pressure gradient across the flute span (delta C_p/delta y) of 0.0029/in. for the first active flute, and 0.0014/in. for all other flutes; this corresponds to a delta C_p of 0.2 and 0.1 across the flute span, respectively. Baffles are staggered chordwise to prevent continuous loss of suction along streamlines (Fig. 23).

Ducts - The skin-flute suction panels were attached to large aluminum ducts (Fig. 24). Duct volumes are presented in Table 4. Cap screws were installed from the duct bottom through the duct wall to threaded aluminum inserts (Fig. 25) located in inactive flutes (Fig. 19). Aluminum insert strength was pull tested and found to be about 690 pounds (which is higher than a worst case 450 pound load). Helicoils were installed in duct walls to help secure the skin-flute panel to the duct substrate.

To help ensure outside model contour, a shim was placed between the suction panel and the aluminum ducting. The liquid shim is shown in Figure 8. The shim was formed by appying liquid epoxy (EA 934) to the suction panel backside and a separator film to the duct wall contact area. Panel and duct are brought together on the master tool until the liquid shim sets after which they can be separated and rejoined without affecting model contour.

The aft panel duct contact surface was remachined to correct for a slight spanwise bow.

Finally, the three duct substrates were leak checked and potential leak paths sealed with RTV 732.

Flaps - The model has three independent, remotely controlled flaps over the aft 10.9 percent chord which provide a means for altering pressure distribution. Flaps are held to the aft upper substrate duct with brackets and are hand-fitted to the duct and to each other. Flaps have no suction control.

Fitting - Upper and lower LFC panels and flaps were jig-bored and bench-fit to a new variable sweep wing box (Fig. 26). Three small filler strips, fit-poured from Hysol 934, were mated to joints between the forward and center panel, center and aft panel, and the aft panel and flap sections. Joints were hand polished to a very smooth finish. Hysol 934 was chosen as the filler material from test results of surface smoothness, temperature cycling, and pressure-tightness. Experiments were made on small panels that simulated model joints. The completed perforated panels mounted on the wing box are shown in Figure 27.

INSTRUMENTATION

The EBP titanium panels are heavily instrumented with surface thin-film gages, surface pressures, surface and flute Kulite gages, and duct pressure tubes and thermocouples. This work was performed at Langley.

Thin Film Gages - Thin film gages are the primary means for detecting model transition location on the perforated model. The gage used is manufactured by Thermo-Systems, Inc. and is composed of a teflon coated wire sensor across the end of an aluma coated 0.0625 in. outer diameter quartz rod. The gage measures temperature difference when flow state changes from laminar to transitional. Thirty-two gages are located on the model as shown in Figure 28, and

tabulated in Table 5. Five thin films are located in the forward panel, seven in the center panel, seventeen in the aft panel and three in the flaps. The surface of a typical thin film gage is shown in Figure 29. Gages are mounted flush with the model surface. Details of gage operation are given in Reference 32.

Surface Pressures - Provision was made for ninety-two surface pressure measurements to verify theoretical chordwise pressure distribution and to check for spanwise pressure variations due to model and tunnel liner variations. Locations are shown in Figure 28, and tabulated in Table 6 (locations 28, 29, 50, 51, 52 and 72 were not implemented because of nearness to the leading edge or welds). All pressure installations were located in the non-suction flutes. The electron-beam perforations provided the air passage to the internal surface where pressure tubes were fastened to the underside of the titanium skin (Fig. 30).

Before the titanium/flute bond was made, holes were drilled in the fiberglass flute structure for tube installation. These holes were temporarily filled with RTV silicon plugs. The skin was bonded to the flutes and the cured RTV helped prevent adhesive flow into skin perforations. RTV was then removed allowing access to the open EBP holes. The end of the pressure tube, which has a sliding collar, was coated with sealant and inserted into the hole. Excess sealant was pushed out, forming a small sealing ring held in place with the sliding collar. After the sealant set, the base of the tube was covered with EA 934 structural adhesive. Figure 30 also shows the completed installation.

Stainless steel pressure tubes 0.093 in. ID by 0.125 in. OD were fastened to the titanium skin underside. Since only about 10 perforations were available to a single pressure tube, occasional hole clogging from adhesive residue or manufacturing defects blocked pressure communication to the tube (Fig. 31). Also, numerous tubes were found to leak. In these instances, a 0.01 in. diameter hole, or 0.02 in. on the aft panel, (a size small enough to avoid disturbing the flow) was drilled through the surface and a 0.04 in. ID by 0.06 in. OD stainless steel tube placed below the surface and bonded in place with EA-934 adhesive. The surface adjoining these pressure orifices was hand polished to a very smooth finish. Of the 92 surface locations, approximately 39 had holes drilled through the surface. These are noted by asterisks in Table 6. No surface pressure tubes had to be replaced on the center panel, suggesting that problems with original tubes were likely due to workmanship and resin flow rather than design.

Flute Pressures - Twenty-one flutes contain a 0.06 in. OD stainless steel pressure tube to measure the flute static pressure as an aid in determining if outflow exists. Flute and surface pressure instrumentation exit the tunnel through flute sidewalls. Flute pressure tubes are located in active flutes 2, 4, 8, 11, 13, 15, 19, 25, 29, 35, 42, 46, 51, 55, 59, 63, 66, 68, 70, 72, and 74.

Acoustic Instrumentation - Eight surface and eight flute Kulite gages were installed in the model to measure surface noise intensity

and noise level below the model boundary layer (after passing through the titanium skin). Location of the Kulite gages is given in Figure 28 and tabulated in Table 7. A photograph of a typical Kulite gage is shown in Figure 32. The sketch in Figure 33 shows how the Kulite gages are mounted.

After model surface instrumentation was installed, clear plastic templates were laid over the panels. Surface pressure taps, thin films, and Kulite gages were located on the templates to enable easy identification of surface instrumentation during model test preparation and tunnel down-time periods.

Nozzles - Fifty-nine axisymmetric aluminum nozzles (Fig. 34) manufactured at Langley are located in the ducts (Fig. 35, Table 4) to move flow from the model to the tunnel suction system. The entrance lip to each nozzle (Fig. 35) is specially designed and machined smooth to insure attached nozzle flow. Twenty-seven nozzles are in the laminar center ducts and thirty-two nozzles are in the adjoining side turbulent ducts (Fig. 36). Individual nozzles were generally designed to limit maximum flow velocity to 224 ft./sec. (0.28 M) to help ensure non-choked flow and avoid possible duct pressure oscillations. Figure 37 shows nozzle length/diameter requirements to avoid choking the flow after model exit. Nozzle dimensions, mass flow rates, design velocities, and pressure drops at design conditions are given in Table 8. Laminar nozzles UL15, LL20, and UL20 were the largest nozzles that would fit in their ducts. From velocity calculations, these nozzles may approach choked flow. However, calculations are based on conservative assumptions, so it is still possible that choking in these nozzles may be avoided. Nozzle inside diameter was measured and serial numbers stamped on the nozzle to facilitate later identification. To avoid additional costs in time and money associated with fabrication of complex two-dimensional nozzles, only cast axisymmetric nozzles were used. Analytical calculations showed axisymmetric nozzles acceptible in all cases. Laminar ducts 1-15 have one nozzle and laminar ducts 16-21 have two nozzles. The laminar nozzles are located near the turbulent bulkheads to avoid flow circulation behind the nozzle, increase flow capability, and help prevent choking. Ducts where turbulent flow is expected each have one nozzle (Fig. 36). Nozzle ends are fitted with gun-bored aluminum cylindrical extension rods sealed at the duct exit to help ensure a leak-free system in transporting flow to the tunnel suction system.

Each nozzle and duct contain a static pressure tap for mass flow rate calculations. Nozzle throat static pressure taps are 0.040 in. OD by 0.034 in. ID stainless steel tubes. Duct static pressure measurements are taken with 0.09 in. OD tubes. In the laminar ducts, three 0.04 in. diameter holes are drilled in the tubes approximately 4 in. apart with the first located at a position 10 times nozzle inner diameter (referenced to the nozzle entrance). In turbulent ducts, one 0.02 in. diameter hole is located halfway between the nozzle entrance and the bulkhead separating the laminar and turbulent ducts. Nozzle and static pressure tap codes versus duct are tabulated in Table 4. Duct instrumentation exits the

tunnel through the duct sidewalls (Fig. 35, 36).

Thermocouples - Duct temperature measurements for mass-flow calculations are obtained with chromel-alumel thermocouples. There are 4 thermocouples in the forward panel, 2 in the center panel and 6 in the aft panel (Fig. 35, 36, Table 4). Shielded (metal) thermocouple wire is used for temperature sensing. The metal shield permits a good exit seal through the duct sidewall. Earlier tests had shown that the porous nature of unshielded thermocouple wire insulation would allow a leak path in the thermocouple from the duct to the tunnel environment. Location of duct thermocouples is listed in Table 4.

A list of drawings used in the model fabrication is included as Table 9.

CONCLUDING REMARKS

Perforated LFC suction panels of approximately 7 foot chord and 7 foot span were fabricated to meet laminar flow control smoothness and waviness specifications using techniques applicable to modern aircraft production lines. The fabrication represents the demonstration of a new LFC structural technology. Electron-beam perforated titanium skin is used as the suction surface. Manufacturing tolerances achieved are considerably improved relative to current production line practice for turbulent aircraft. Critical issues related to large suction panel manufacturing were identified and largely resolved.

REFERENCES

1. Bushnell, D. M.; and Tuttle, M. H.: Survey and Bibliography on Attainment of Laminar Flow Control in Air Using Pressure Gradient and Suction - Volume I. NASA RP-1035, 1979.

2. Bushnell, D. M.; and Tuttle, M. H.: Survey and Bibliography on Attainment of Laminar Flow Control in Air Using Pressure Gradient and Suction - Volume II. NASA RP-1035, 1979.

3. Jobe, C. E.: A Bibliography of AFFDL/FXM Reports on Laminar Flow Control. AFFDL-RM-76-26-FXM, U.S. Air Force, 1976.

4. Tuttle, M. H.; and Maddalon, D. V.: Laminar Flow Control 1976-1982; A Selected, Annotated Bibliography. NASA TM-84496, 1982.

5. Braslow, A. L.; Burrows, D. L.; Teterzin, N.; and Visconti, F.: Experimental and Theoretical Studies of Area Suction for the Control of the Laminar Boundary Layer on a NACA 64A010 Airfoil, NACA Report 1025, 1951.

6. Antonatos, P. P.: Laminar Flow Control - Concepts and Applications. Astronautics and Aeronautics, July 1966.

7. Nenni, J. P.; and Gluyas, G. L.: Aerodynamic Design and Analysis on an LFC Surface. Astronautics and Aeronautics, July 1966.

8. White, R. C.; Sudderth, R. W.; and Wheldan, W. G.: Laminar Flow Control on the X-21. Astronautics and Aeronautics, July 1966.

9. Pfenninger, W.; and Reed, V. D.: Laminar Flow Research and Experiments. Astronautics and Aeronautics, July 1966.

10. Lachmann, G. V.: Boundary Layer Control. Journal of the Royal Aeronautical Society, Vol. 59, No. 531, pp. 163-198, Mar. 1955.

11. Sturgeon, R. F.; et al.: Study of the Application of Advanced Technologies to Laminar-Flow Control Systems for Subsonic Transports. NASA CR-144949, 1976.

12. Anon; Douglas Aircraft Co. Staff: Evaluation of Laminar Flow Control System Concepts for Subsonic Commercial Transport Aircraft. NASA CR-159251, 1983.

13. Anon; Douglas Aircraft Co. Staff: Laminar Flow Control Leading Edge Glove Flight Test Article Development. NASA CR-172137, 1984.

14. Anderson, C. B.; et al.: Development of Laminar Flow Control Wing Surface Porous Structure. NASA CR-172424, 1984.

15. Goldsmith, John: Critical Laminar Suction Parameters for Suction into an Insulated Hole or Single Row of Holes. Rep. No. BLC-95, Rep. No. NAI-57-529, Northrop Aircraft Inc., Feb. 1957.

16. Reynolds, G.A. and Saric, W. S.: Experiments on the Stability of the Flat-Plate Boundary Layer with Suction. AIAA 82-1026, 1982.

17. Saric, W. S. and Reed, H.L.: Effect of Suction and Blowing on Boundary Layer Transition. AIAA 83-0043, 1983.

18. Wagner, R. D.: Laminar Flow Integration-Flight Tests Status and Plans. NASA CP-2397, 1985.

19. Pfenniger, W.; Reed, H. L.; and Dagenhart, J. R.: Design Considerations of Advanced Supercritical Low Drag Suction Airfoils. Viscous Flow Drag Reduction, Vol. 72, Progress in Astronautics and Aeronautics, 1980.

20. Reed, H.L. and Nayfeh, A.H.: Stability of Flow over Plates with Porous Suction Strips. AIAA 81-1280, 1981.

21. Dagenhart, J. R.: Amplified Crossflow Disturbances in the Laminar Boundary Layer on Swept Wings With Suction. NASA TP-1902, 1981.

22. Anon.: Boeing Commercial Aircraft Company Staff, Hybrid Laminar Flow Control Study. NASA CR-165930, 1982.

23. Maddalon, D. V.; and McMillin, M. L.: Effect of Surface Waviness on a Super-Critical Laminar Flow Control Airfoil. NASA TM-85705, 1983.

24. Wagner, R. D.; Maddalon, D. V.; and Fischer, M. C.: Technology Developments for Laminar Boundary Layer Control on Subsonic Transport Aircraft. AGARD CP-265, 1984.

25. Anon.: Boeing Commercial Aircraft Company Staff, F-111 Natural Laminar Flow Glove Flight Test Data Analysis and Boundary Layer Stability Analysis. NASA CR-166051, 1984.

26. Braslow, A. L.; and Fischer, M. C.: Design Considerations for Application of Laminar Flow Control Systems to Transport Aircraft. Presented at the AGARD/FOP VKI Special Course on "Aircraft Drag Prediction and Reduction." Brussels, Belgium. May 20-23, 1985.

27. Maddalon, D. V.; and Wagner, R. D.: Operational Considerations for Laminar Flow Aircraft. Laminar Flow Aircraft Certification, NASA CP-2413, 1986.

28. Bobbitt, P. J.; et al.: A Faster "Transition" to Laminar Flow. SAE Paper 851855, 1985.

29. Newman, P. A.; Anderson, E. C.; and Peterson, J. B. Jr.: Aerodynamic Design of the Contoured Wind-Tunnel Liner for the NASA Supercritical, Laminar-Flow-Control, Swept-Wing Experiment. NASA TP-2335, 1984.

30. Harvey W. D.; and Pride, J. D.: The NASA Langley Laminar Flow Control Experiment. AIAA 82-0567, 1982.

31. Berry, S. A.: Incompressible Boundary-Layer Stability Analysis of LFC Experimental Data. Master of Science Thesis, George Washington University, Jan. 1986.

32. Obara, C. J.; and Holmes, B. J.: Flight-Measured Laminar Boundary-Layer Transition Phenomena Including Stability Theory Analysis. NASA TP-2417, 1985.

TABLE 1 - CENTERLINE PRESSURE DATA

R = 20 X 10^6, M = 0.755

ACTIVE FLUTE NO.	MASS FLOW RATE lbm/sec	SURFACE Ps,Psfa	FLUTE Pf,Psfa	DUCT Pd,Psfa	Ps-Pf Psf	Pf-Pd Psf	Ps-Pd Psf
1	.00262	694.63	688.75	586.12	5.88	102.63	108.51
2	.00262	701.73	695.61	586.12	6.12	109.49	115.61
3	.00428	702.48	697.07	616.48	5.91	80.59	86.50
4	.00428	705.44	699.49	616.48	5.95	83.01	88.96
5	.00428	709.16	703.10	616.48	6.06	86.62	92.68
6	.00419	709.70	703.94	623.76	5.76	80.18	85.94
7	.00419	711.72	705.90	623.76	5.82	82.14	87.96
8	.00419	713.74	707.86	623.76	5.88	84.10	89.98
9	.00410	714.96	709.18	630.59	5.78	78.59	84.37
10	.00410	716.47	710.64	630.59	5.83	80.05	85.88
11	.00410	717.98	712.10	630.59	5.88	81.51	87.39
12	.00267	716.93	711.06	632.76	5.87	78.30	84.17
13	.00267	718.13	712.22	632.76	5.91	79.46	85.37
14	.00394	721.00	715.20	637.54	5.80	77.66	83.46
15	.00394	721.99	716.16	637.54	5.83	78.62	84.45
16	.00394	722.98	717.11	637.54	5.86	79.57	85.43
17	.00524	723.96	718.19	640.23	5.78	77.96	83.74
18	.00524	724.66	718.86	640.23	5.80	78.63	84.43
19	.00524	725.36	719.54	640.23	5.82	79.31	85.13
20	.00524	726.06	720.21	640.23	5.84	79.98	85.82
21	.00750	726.94	721.19	640.72	5.76	80.47	86.23
22	.00750	727.40	721.63	640.72	5.77	80.91	86.68
23	.00750	727.86	722.08	640.72	5.78	81.36	87.14
24	.00750	728.32	722.52	640.72	5.80	81.80	87.60
25	.00750	728.78	722.97	640.72	5.81	82.25	88.06
26	.00750	729.24	723.41	640.72	5.83	82.69	88.52
27	.00709	730.26	724.55	645.51	5.71	79.04	84.75
28	.00709	730.75	725.02	645.51	5.73	79.51	85.24
29	.00709	731.24	725.50	645.51	5.74	79.99	85.73
30	.00709	731.74	725.98	645.51	5.76	80.47	86.23
31	.00709	732.23	726.46	645.51	5.77	80.95	86.72
32	.00709	732.72	726.93	645.51	5.79	81.42	87.21
33	.00678	733.35	727.59	648.72	5.76	78.87	84.63
34	.00678	733.55	727.78	648.72	5.77	79.06	84.83
35	.00678	733.75	727.97	648.72	5.78	78.25	85.03
36	.00678	733.95	728.17	648.72	5.78	79.45	85.23
37	.00678	734.15	728.36	648.72	5.79	79.64	85.43
38	.00678	734.35	728.55	648.72	5.80	79.83	85.63
39	.00535	733.58	727.79	648.11	5.79	79.68	85.47
40	.00535	733.59	727.80	648.11	5.79	79.69	85.48
41	.00535	733.61	727.82	648.11	5.79	79.71	85.50
42	.00535	733.63	727.84	648.11	5.79	79.73	85.52
43	.00535	733.64	727.85	648.11	5.79	79.74	85.53

TABLE 1 - CONCLUDED

ACTIVE FLUTE NO.	MASS FLOW RATE lbm/sec	SURFACE Ps,Psfa	FLUTE Pf,Psfa	DUCT Pd,Psfa	Ps-Pf Psf	Pf-Pd Psf	Ps-Pd Psf
44	.00562	733.32	727.53	646.06	5.79	81.47	87.26
45	.00562	733.32	727.53	646.06	5.79	81.47	87.26
46	.00562	733.32	727.53	646.06	5.79	81.47	87.26
47	.00562	733.32	727.53	646.06	5.79	81.47	87.26
48	.00562	733.32	727.53	646.06	5.79	81.47	87.26
49	.00409	733.64	727.85	647.13	5.79	80.72	86.51
50	.00409	733.65	727.86	647.13	5.79	80.73	86.52
51	.00409	733.67	727.88	647.13	5.79	80.75	86.74
52	.00409	733.68	727.89	647.13	5.79	80.76	86.75
53	.00469	734.02	728.29	644.69	5.72	83.60	89.32
54	.00469	734.46	728.72	644.69	5.74	84.03	89.77
55	.00469	734.90	729.15	644.69	5.75	84.46	90.21
56	.00469	735.34	729.58	644.69	5.76	84.89	90.65
57	.00469	735.78	730.01	644.69	5.77	85.32	91.09
58	.02157	736.97	703.09	677.95	33.87	25.14	59.01
59	.02157	739.37	704.59	677.95	34.78	26.64	61.42
60	.02157	741.77	706.09	677.95	35.68	28.14	63.82
61	.02157	744.17	707.62	677.95	36.55	29.67	66.22
62	.02346	750.43	697.55	697.75	51.89	0.80	52.69
63	.02346	755.59	698.72	697.75	56.87	0.97	57.84
64	.02346	760.75	698.91	697.75	61.83	1.16	62.99
65	.02260	764.81	717.28	716.59	47.53	0.69	48.22
66	.02260	733.35	717.56	716.59	55.79	0.97	56.76
67	.02260	781.89	717.90	716.59	63.99	1.31	65.30
68	.01468	792.99	747.83	747.17	45.16	0.66	45.82
69	.01468	811.51	748.51	747.17	63.00	1.34	64.34
70	.01454	835.47	784.05	783.09	51.42	0.96	52.38
71	.01454	864.32	814.23	783.09	50.09	31.14	81.23
72	.01375	896.29	848.45	847.49	47.84	0.96	48.80
73	.01375	927.30	880.23	847.49	47.07	32.74	79.81
74	.01343	954.76	909.11	908.14	45.65	0.97	46.62

TABLE 2 - DUCT AND FLUTE LOCATIONS

PANEL	DUCT (LAM.)	DUCT (TURB.)	FLUTE	X/C FLUTE CENTER	METERING HOLE DIAMETER (IN.)	NO. OF HOLES PER FLUTE PARTITIONED REGION
1	1	1	1	0.034	0.024	1
1	1	1	2	0.050	0.024	1
1	2	1	3	0.059	0.026	1
1	2	1	4	0.062	0.026	1
1	2	1	5	0.081	0.026	1
1	3	2	6	0.089	0.026	1
1	3	2	7	0.101	0.026	1
1	3	2	8	0.112	0.026	1
1	4	2	9	0.124	0.026	1
1	4	2	10	0.135	0.026	1
1	4	2	11	0.147	0.026	1
1	5	3	12	0.158	0.026	1
1	5	3	13	0.169	0.026	1
1	6	3	14	0.181	0.026	1
1	6	3	15	0.192	0.026	1
1	6	3	16	0.204	0.026	1
1	7	4	17	0.217	0.026	1
1	7	4	18	0.228	0.026	1
1	7	4	19	0.238	0.026	1
1	7	4	20	0.249	0.026	1
2	8	5	21	0.265	0.026	1
2	8	5	22	0.276	0.026	1
2	8	5	23	0.287	0.026	1
2	8	5	24	0.297	0.026	1
2	8	5	25	0.308	0.026	1
2	8	5	26	0.318	0.026	1
2	9	6	27	0.333	0.026	1
2	9	6	28	0.344	0.026	1
2	9	6	29	0.356	0.026	1
2	9	6	30	0.367	0.026	1
2	9	6	31	0.379	0.026	1
2	9	6	32	0.390	0.026	1
2	10	7	33	0.402	0.026	1
2	10	7	34	0.414	0.026	1
2	10	7	35	0.425	0.026	1
2	10	7	36	0.437	0.026	1
2	10	7	37	0.448	0.026	1
2	10	7	38	0.460	0.026	1

TABLE 2 - CONCLUDED

PANEL	DUCT (LAM.)	DUCT (TURB.)	FLUTE	X/C FLUTE CENTER	METERING HOLE DIAMETER (IN.)	NO. OF HOLES PER FLUTE PARTITIONED REGION
2	11	8	39	0.471	0.026	1
2	11	8	40	0.483	0.026	1
2	11	8	41	0.494	0.026	1
2	11	8	42	0.506	0.026	1
2	11	8	43	0.517	0.026	1
2	12	9	44	0.532	0.026	1
2	12	9	45	0.544	0.026	1
2	12	9	46	0.555	0.026	1
2	12	9	47	0.567	0.026	1
2	12	9	48	0.578	0.026	1
3	13	10	49	0.594	0.026	1
3	13	10	50	0.605	0.026	1
3	13	10	51	0.616	0.026	1
3	13	10	52	0.626	0.026	1
3	14	11	53	0.635	0.026	1
3	14	11	54	0.646	0.026	1
3	14	11	55	0.658	0.026	1
3	14	11	56	0.669	0.026	1
3	14	11	57	0.681	0.026	1
3	15	12	58	0.692	0.113	4
3	15	12	59	0.703	0.113	4
3	15	12	60	0.715	0.113	4
3	16	13	61	0.726	0.113	4
3	16	13	62	0.744	0.161	60
3	16	13	63	0.755	0.161	60
3	16	13	64	0.767	0.161	60
3	17	14	65	0.778	0.161	58
3	17	14	66	0.790	0.161	58
3	17	14	67	0.801	0.161	58
3	18	15	68	0.813	0.161	56
3	18	15	69	0.824	0.161	56
3	19	15	70	0.836	0.161	54
3	19	15	71	0.847	0.104	21
3	20	16	72	0.857	0.154	56
3	20	16	73	0.869	0.100	22
3	21	16	74	0.881	0.161	49

TABLE 3 – TURBULENT REGION FLUTE SUCTION WIDTH

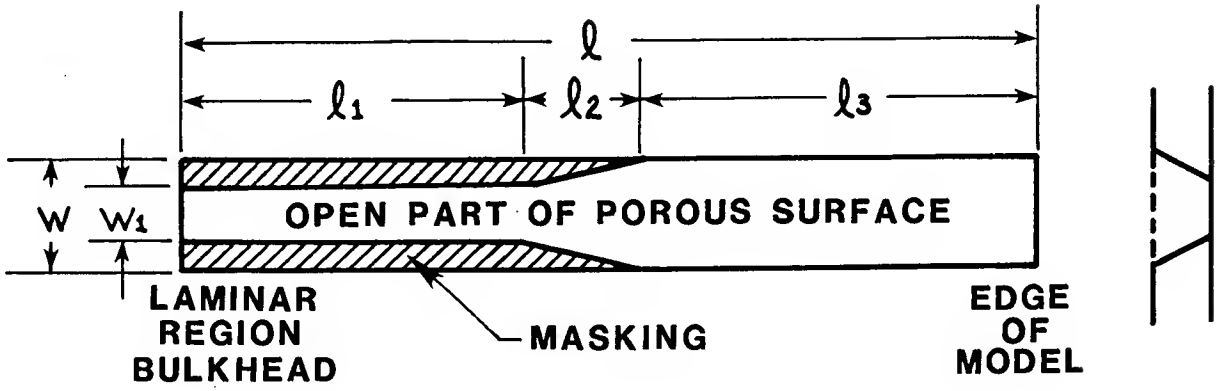

SIDE	DUCT NO.	X/C CENTER OF DUCT	$\frac{W_1}{W}$ RAMP	$\frac{\ell_1}{\ell}$ BOTTOM	$\frac{\ell_2}{\ell}$ RAMP	$\frac{\ell_3}{\ell}$ RAMP TOP
CEILING	11	.664	.897	.196	.154	.650
	12	.718	.805	.325	.212	.463
	13	.759	.754	.420	.236	.344
	14	.799	.716	.480	.237	.283
	15	.837	.692	.503	.229	.268
	16	.873	.676	.513	.224	.263
FLOOR	11	.664	.897	.183	.097	.720
	12	.718	.805	.299	.195	.506
	13	.759	.754	.364	.226	.410
	14	.799	.716	.412	.240	.348
	15	.837	.692	.450	.234	.316
	16	.873	.676	.473	.229	.298

TABLE 4 - DUCT INSTRUMENTATION

LAMINAR DUCT

DUCT	NOZZLE	NOZZLE STATIC	DUCT STATIC	THERMO-COUPLE	VOLUME (CU. IN.)
1	LL 1	LL 1N	LL 1S	ITC1	80.1
2	UL 2	UL 2N	UL 2S		106.0
3	LL 3	LL 3N	LL 3S		136.8
4	UL 4	UL 4N	UL 4S		155.4
5	LL 5	LL 5N	LL 5S		89.0
6	UL 6	UL 6N	UL 6S		153.1
7	LL 7	LL 7N	LL 7S	7TC4	146.8
8	UL 8	UL 8N	LL 8S		305.6
9	LL 9	LL 9N	LL 9S		408.7
10	LL 10	LL 10N	LL 10S		398.2
11	UL 11	UL 11N	UL 11S		257.0
12	LL 12	LL 12N	LL 12S	12TC6	318.1
13	LL 13	LL 13N	LL 13S		138.5
14	UL 14	UL 14N	UL 14S		300.2
15	UL 15	UL 15N	UL 15S		261.6
16	LL 16, UL 16	LL 16N, UL 16N	LL 16S, UL 16S	16TC7	158.7
17	LL 17, UL 17	LL 17N, UL 17N	LL 17S, UL 17S		142.3
18	LL 18, UL 18	LL 18N, UL 18N	LL 18S, UL 18S	18TC9	73.0
19	LL 19, UL 19	LL 19N, UL 19N	LL 19S, UL 19S		55.1
20	LL 20, UL 20	LL 20N, UL 20N	LL 20S, UL 20S	20TC11	43.4
21	LL 21, UL 21	LL 21N, UL 21N	LL 21S, UL 21S		28.8

UPPER TURBULENT DUCT

1	UT 1	UT 1N	UT 1S	ITC2	15.8
2	UT 2	UT 2N	UT 2S		29.2
3	UT 3	UT 3N	UT 3S		26.6
4	UT 4	UT 4D	UT 4S	4TC3	20.6
5	UT 5	UT 5N	UT 5S		36.9
6	UT 6	UT 6N	UT 6S		60.1
7	UT 7	UT 7N	UT 7S		65.7
8	UT 8	UT 8N	UT 8S		57.0
9	UT 9	UT 9N	UT 9S	9TC5	57.1
10	UT 10	UT 10N	UT 10S		40.1
11	UT 11	UT 11N	UT 11S		79.8
12	UT 12	UT 12N	UT 12S		65.5
13	UT 13	UT 13N	UT 13S		42.8
14	UT 14	UT 14N	UT 14S		39.9
15	UT 15	UT 15N	UT 15S	15TC8	41.3
16	UT 16	UT 16N	UT 16S	16TC10	23.0

TABLE 4 - CONCLUDED

LOWER TURBULENT DUCT

DUCT	NOZZLE	NOZZLE STATIC	DUCT STATIC	VOLUME (CU. IN.)
1	LT 1	LT 1N	LT 1S	23.0
2	LT 2	LT 2N	LT 2S	62.6
3	LT 3	LT 3N	LT 3S	32.0
4	LT 4	LT 4N	LT 4S	21.8
5	LT 5	LT 5N	LT 5S	53.3
6	LT 6	LT 6N	LT 6S	78.3
7	LT 7	LT 7N	LT 7S	86.8
8	LT 8	LT 8N	LT 8S	89.9
9	LT 9	LT 9N	LT 9S	93.6
10	LT 10	LT 10N	LT 10S	39.5
11	LT 11	LT 11N	LT 11S	97.6
12	LT 12	LT 12N	LT 12S	93.3
13	LT 13	LT 13N	LT 13S	51.7
14	LT 14	LT 14N	LT 14S	49.2
15	LT 15	LT 15N	LT 15S	51.5
16	LT 16	LT 16N	LT 16S	29.5

NOZZLE CODE

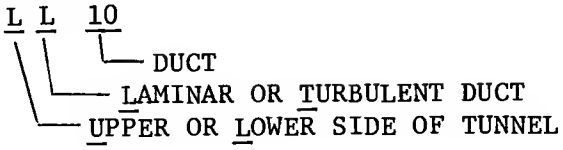

STATIC TAP CODE

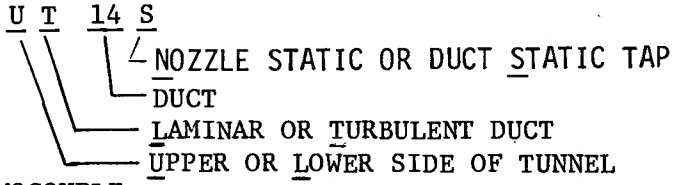

THERMOCOUPLE

TABLE 5 - THIN FILM GAGE LOCATIONS

Forward Panel

No.	X	Y
24	18.05	-12.17
25	2.25	-20.02
26	2.25	-18.77

Center Panel

No.	X	Y
21	44.48	-26.28
22	33.65	-20.12
23	22.90	-15.47
51	33.65	-33.42
52	33.65	-0.42
53	22.90	-29.50
54	22.90	3.27

Aft Panel

No.	X	Y
17	47.81	-35.75
18	47.81	-26.61
19	47.81	-16.04
20	47.81	-2.86
13	56.72	-38.58
14	56.72	-29.45
15	56.72	-18.88
16	56.72	-5.70
8	62.11	5.77
9	62.11	-40.29
10	62.11	-31.15
11	62.11	-20.59
12	62.11	-7.41
4	68.25	-42.50
5	68.25	-33.36
6	68.25	-22.79
7	68.25	-9.61

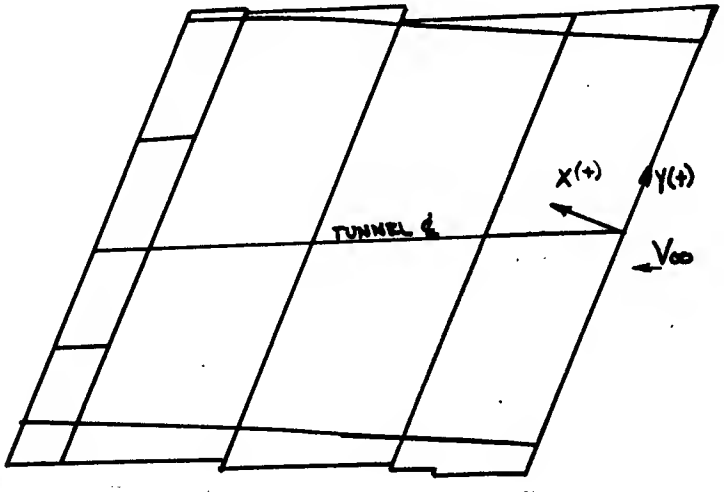

TABLE 6 - SURFACE PRESSURE ORIFICE LOCATIONS

FORWARD PANEL

NO.	X	Y
1*	2.25	32.09
2*	18.05	27.09
10*	2.25	21.43
11*	18.05	16.43
19*	2.25	16.10
20*	18.05	11.10
30*	2.25	4.27
31*	7.41	2.17
32*	12.78	- 1.37
33*	18.05	- 1.03
52*	1.47	- 7.36
53*	2.25	- 8.87
54*	4.73	-12.15
55*	7.41	-10.97
56*	12.78	-14.50
57*	18.05	-14.17
81*	2.25	-23.31
82*	18.05	-28.64
90*	2.25	-38.23
91*	18.05	-43.23

CENTER PANEL

NO.	X	Y
3	3.65	22.13
12	33.65	11.48
21	33.65	6.15
34	22.90	- 4.33
35	28.25	- 4.04
36	33.65	- 8.19
37	37.27	- 7.31
38	42.68	- 8.86
58	22.90	-17.47
59	28.25	-17.18
60	33.65	-21.32
61	37.27	-20.45
62	39.98	-23.12
63	42.68	-21.99
64	44.48	-24.28
83	33.65	-33.26
92	33.65	-48.19

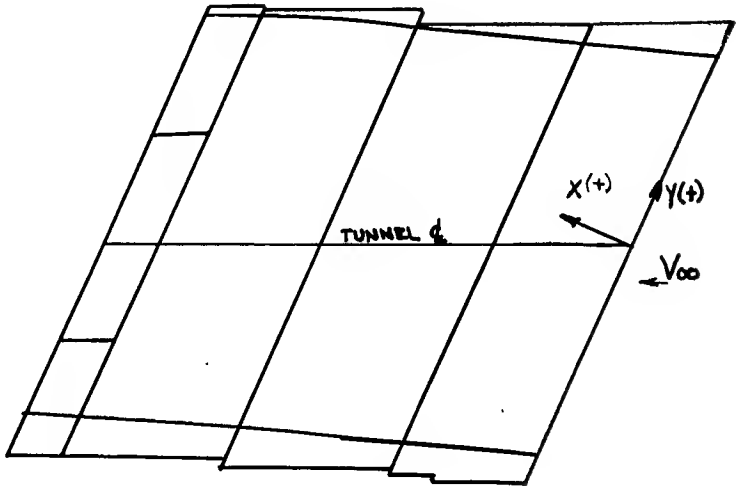

*ORIFICE REPLACED

ALL DIMENSIONS IN INCHES

TABLE 6 - CONCLUDED

AFT PANEL

NO.	X	Y	NO.	X	Y	NO.	X	Y
4	47.81	16.21	70*	54.92	-27.64	17	62.11	2.45
13		6.99	6	55.86	-15.08	26		- 2.88
22		1.66	15	56.72	4.15	46		-16.82
39		-10.28	24		- 1.18	76		-29.95
65		-23.41	43		-13.11	88		-42.29
84		-37.75	71*		-26.25	97		-57.22
93		-52.67	86*		-40.58	77	63.91	-28.59
66	48.64	-26.00	95*		-55.51	47*	65.69	-18.50
40*	50.45	-11.48	44	58.53	-14.05	78		-31.63
67		-23.49	73		-27.19	79	67.43	-30.27
5*	52.25	16.24	7	59.43	14.01	9*	68.25	10.90
14*		6.58	16		3.35	18*		0.24
23*		2.51	25		- 1.97	27*		- 5.09
41*		-13.88	45		-16.11	48*		-19.23
68		-27.02	74		-29.25	80*		-32.36
85		-39.16	87		-41.38	89*		-44.50
94*		-54.08	96		-56.31	98*		-59.42
69	53.13	-25.24	75*	61.20	-27.88			
42	54.92	-14.51	8	62.11	13.10			

*ORIFICE REPLACED

ALL DIMENSIONS IN INCHES

TABLE 7 - KULITE GAGE LOCATIONS

Forward Panel

No.	X	Y
1S	4.73	-6.01
1F	4.73	-7.01
2S	12.78	-9.42
2F	12.78	-10.42
3S	18.84	-11.99
3F	18.84	-12.99

Aft Panel

No.	X	Y
7S	51.35	-25.80
7F	51.35	-26.80
8S	67.43	-32.62
8F	67.43	-33.62

Center Panel

No.	X	Y
4S	26.47	-15.24
4F	26.47	-16.24
5S	35.57	-18.66
5F	35.57	-19.66
6S	43.58	-22.50

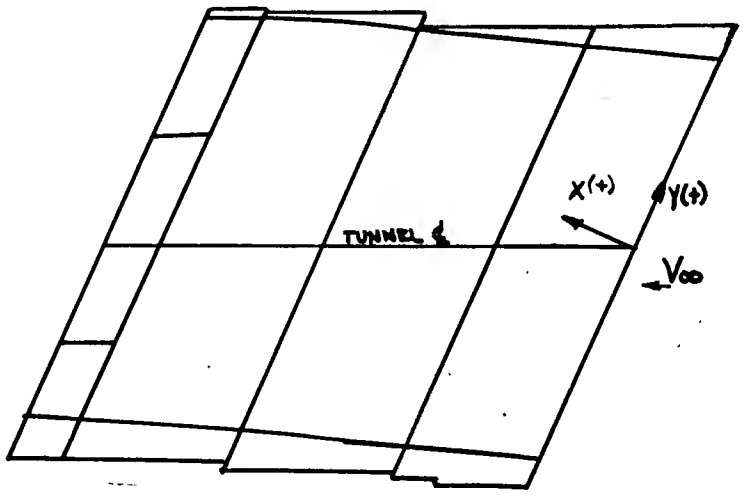

TABLE 8A - LAMINAR NOZZLE PARAMETERS

NOZZLE	DIAMETER (IN.)	LENGTH (IN.)	MASS FLOW RATE (LB/SEC)	VELOCITY (FT/SEC)	$P_{DUCT} - P_{NOZZLE}$ (LBS/FT^2)
LL 1	0.375	18	0.00290	166	10.1
UL 2	0.438	16	0.00469	194	13.9
LL 3	0.438	19	0.00457	187	13.2
UL 4	0.438	16	0.00448	182	12.6
LL 5	0.375	19	0.00295	164	10.1
UL 6	0.438	16	0.00431	174	11.5
LL 7	0.500	19	0.00577	178	12.1
UL 8	0.562	19	0.00826	201	15.5
LL 9	0.562	22	0.00777	188	13.7
LL 10	0.562	22	0.00743	179	12.5
UL 11	0.500	22	0.00585	179	12.4
LL 12	0.500	23	0.00627	191	14.2
LL 13	0.438	24	0.00444	176	12.0
UL 14	0.438	27	0.00516	205	16.3
UL 15	0.875*	27	0.03370	340	43.8
LL 16	0.625	27	0.01070	207	16.7
UL 16	0.625	27	0.01070	207	16.7
LL 17	0.625	27	0.01035	196	15.2
UL 17	0.625	27	0.01035	196	15.2
LL 18	0.500	28	0.00675	192	15.2
UL 18	0.500	27	0.00675	192	15.2
LL 19	0.500	28	0.00660	180	13.8
UL 19	0.500	27	0.00660	180	13.8
LL 20	0.375*	28	0.00645	303	40.7
UL 20	0.375*	27	0.00645	303	40.7
LL 21	0.313	28	0.00320	201	19.1
UL 21	0.313	27	0.00320	201	19.1

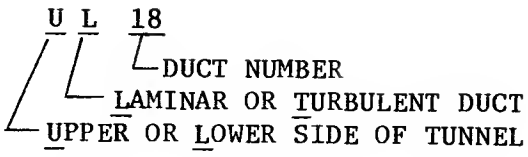

*LARGEST NOZZLE POSSIBLE FOR DUCT

TABLE 8B - TURBULENT NOZZLE PARAMETERS

NOZZLE	INSIDE DIAMETER (IN.)	LENGTH (IN.)	MASS FLOW RATE (LB/SEC)	VELOCITY (FT/SEC)	PRESSURE DROP (LBS/FT^2)
UT 1	0.188	5	0.00102	233	19.9
UT 2	0.250	5	0.00143	180	12.2
UT 3	0.250	5	0.00127	158	9.5
UT 4	0.250	5	0.00109	238	21.7
UT 5	0.250	5	0.00163	200	15.4
UT 6	0.250	5	0.00177	217	18.2
UT 7	0.250	5	0.00193	235	21.5
UT 8	0.250	5	0.00177	216	18.1
UT 9	0.313	5	0.00213	166	10.7
UT 10	0.250	5	0.00153	186	13.5
UT 11	0.313	5	0.00213	165	10.6
UT 12	0.813	5	0.01700	198	15.0
UT 13	0.625	5	0.01410	273	28.9
UT 14	0.625	5	0.01550	293	34.1
UT 15	0.563*	5	0.02210	497	102.0
UT 16	0.375*	5	0.01760	796	294.0
LT 1	0.188	5	0.00070	160	9.4
LT 2	0.188	5	0.00102	227	19.4
LT 3	0.188	5	0.00097	214	17.4
LT 4	0.188	5	0.00091	199	15.0
LT 5	0.188	5	0.00100	218	18.2
LT 6	0.250	5	0.00160	196	14.8
LT 7	0.250	5	0.00175	213	17.7
LT 8	0.250	5	0.00159	194	14.6
LT 9	0.250	5	0.00190	232	20.9
LT 10	0.250	5	0.00170	207	16.7
LT 11	0.313	5	0.00239	185	13.4
LT 12	0.813	5	0.01860	217	17.9
LT 13	0.625	5	0.01550	299	35.0
LT 14	0.625	5	0.01670	258	39.5
LT 15	0.563*	5	0.02370	532	117.3
LT 16	0.375*	5	0.01880	851	335.5

*LARGEST NOZZLE POSSIBLE FOR DUCT

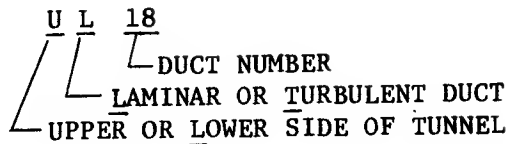

TABLE 9 - PERFORATED LAMINAR FLOW CONTROL

MODEL DRAWINGS

NASA Number	Title
316079	Nozzles - LFC Wing
316548	Flow Nozzle Assembly
316640	Duct, Static Orifice Tube Installation
316758	Panel Installation, LFC Porous Surface
316759	Center Panel, Upper Porous
316760	Forward Panel, Upper Porous
316761	Aft Panel, Upper Porous
316762	Forward Substrate
316763	Center Substrate
316764	Aft Substrate
316765	Nozzle and Instrumentation Installation
316766	Panel/Substrate Assembly
316767	Upper Surface Instrumentation

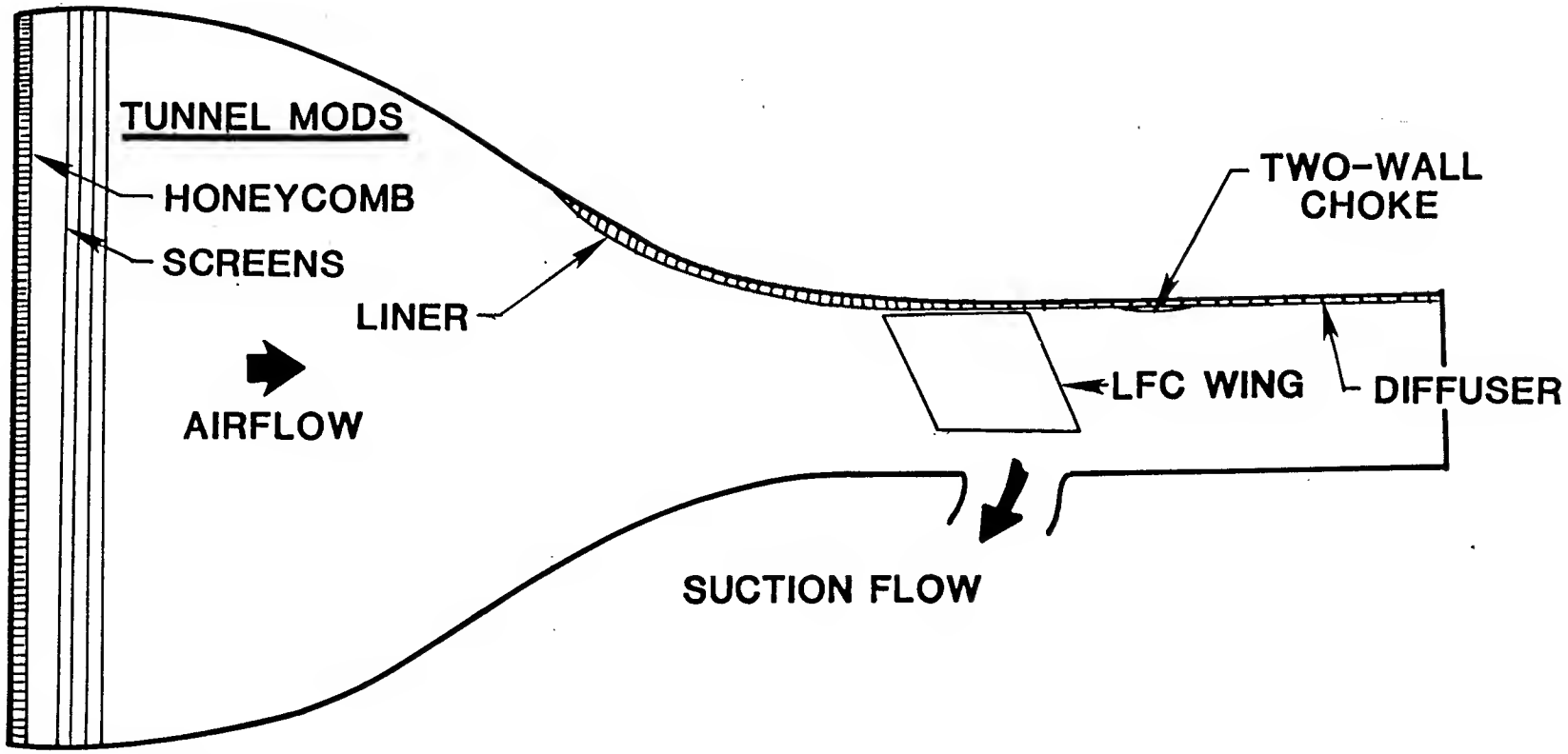

Figure 1. Test setup of laminar flow control wing in 8 ft. tunnel.

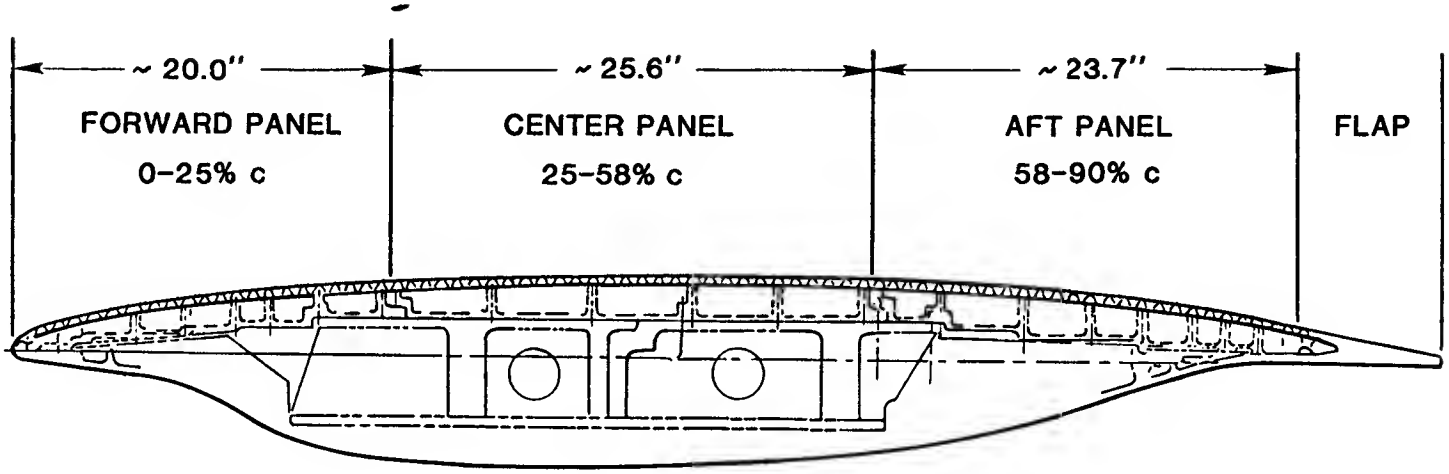

Figure 2. Laminar flow control airfoil.

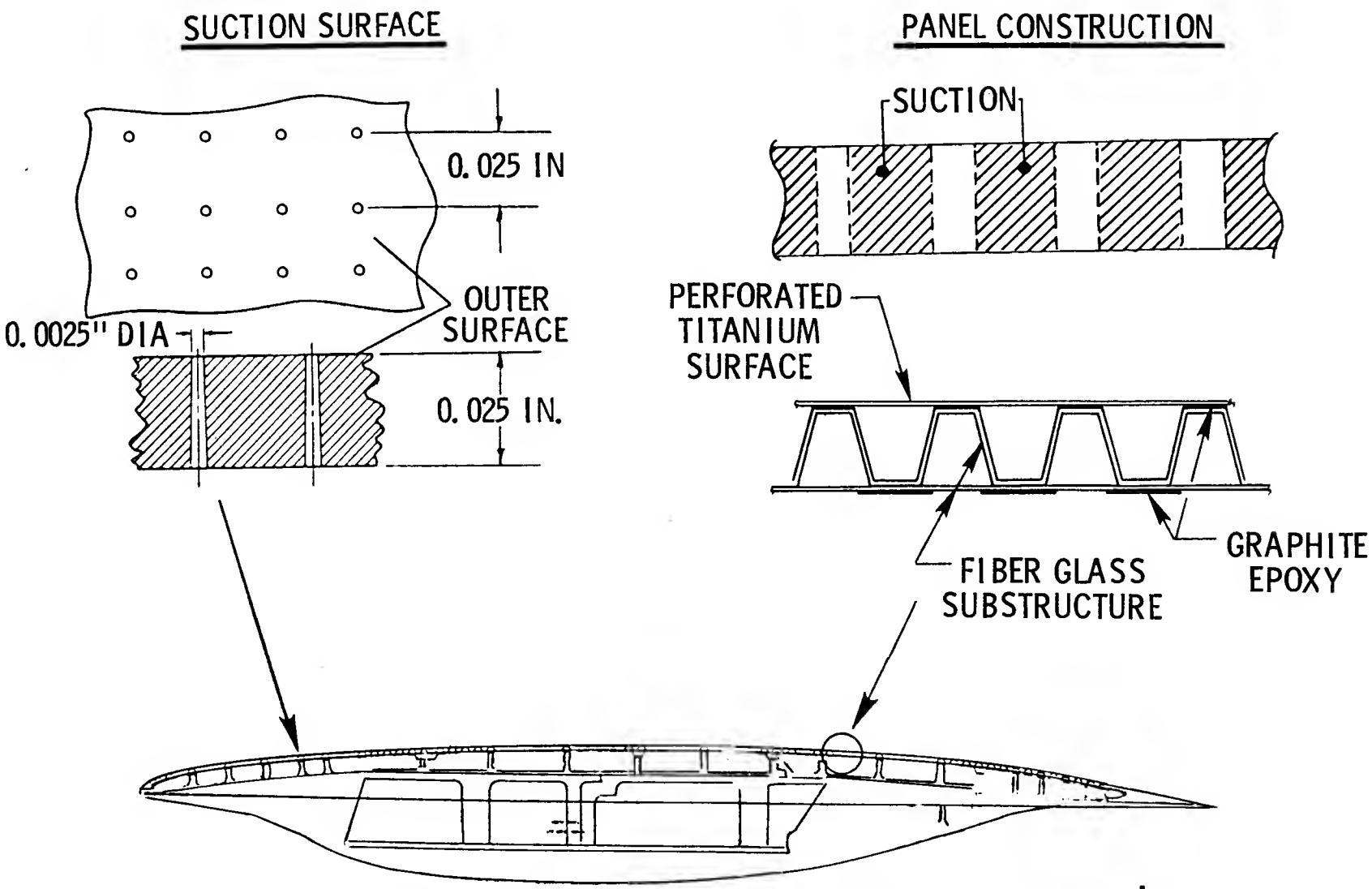

Figure 3. Electron beam perforated titanium panels.

- TRANSITION IS CAUSED BY THE SELECTIVE AMPLIFICATION OF BOUNDARY LAYER DISTURBANCES

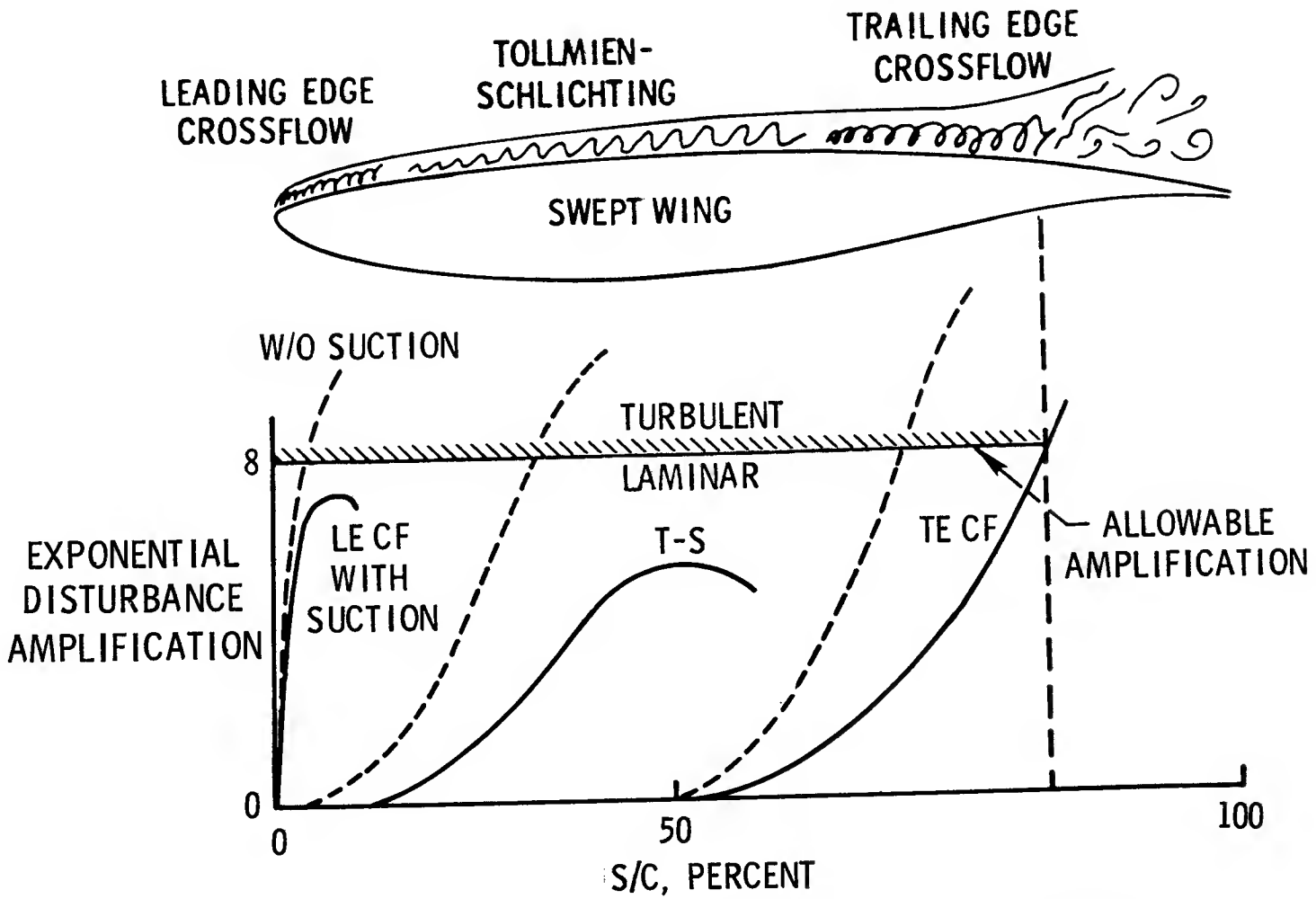

Figure 4. Boundary layer stability and transition.

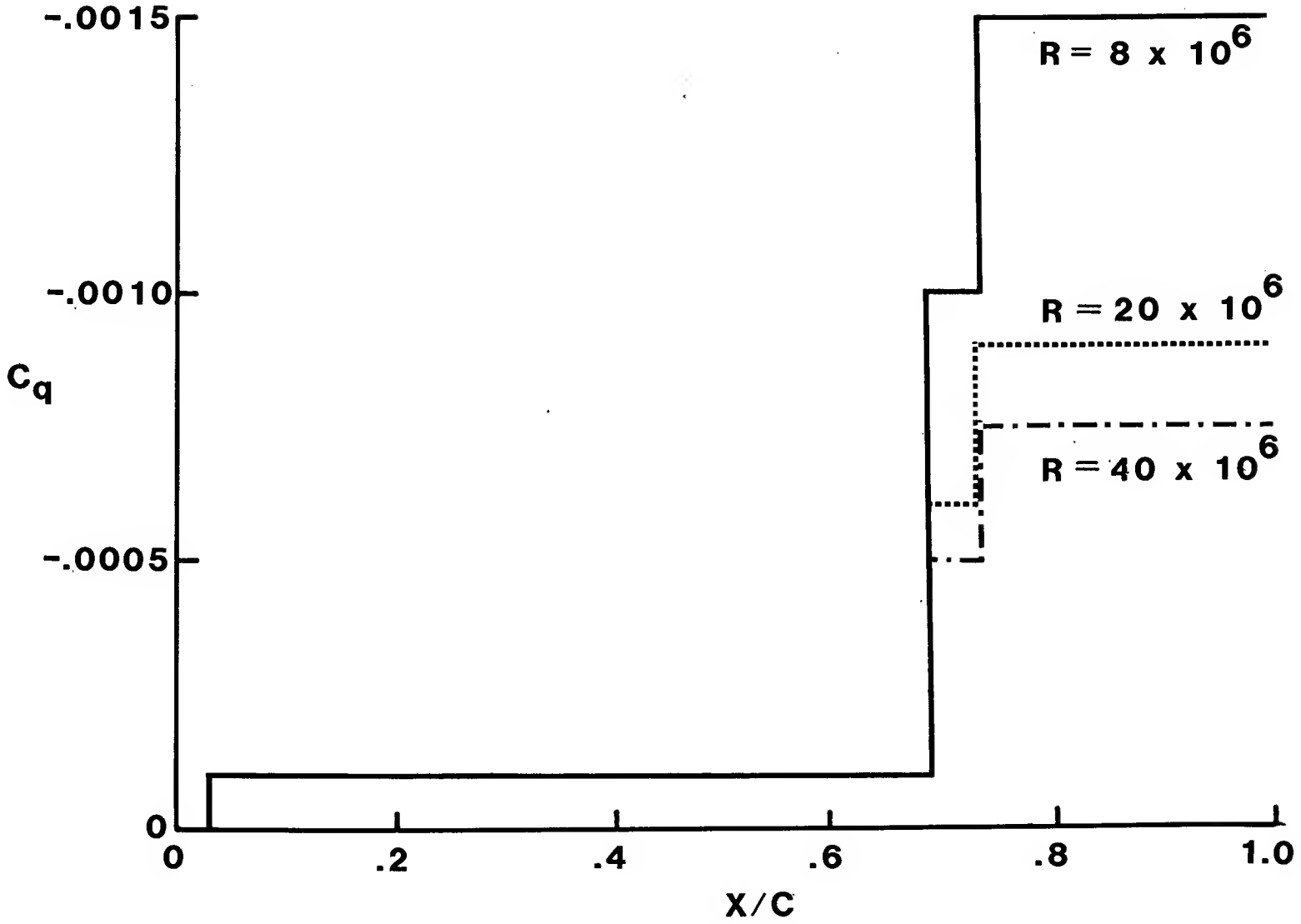

Figure 5. Suction coefficient versus Reynolds number.

REQUIRED: NO OUTFLOW AT MINIMUM SUCTION LEVEL

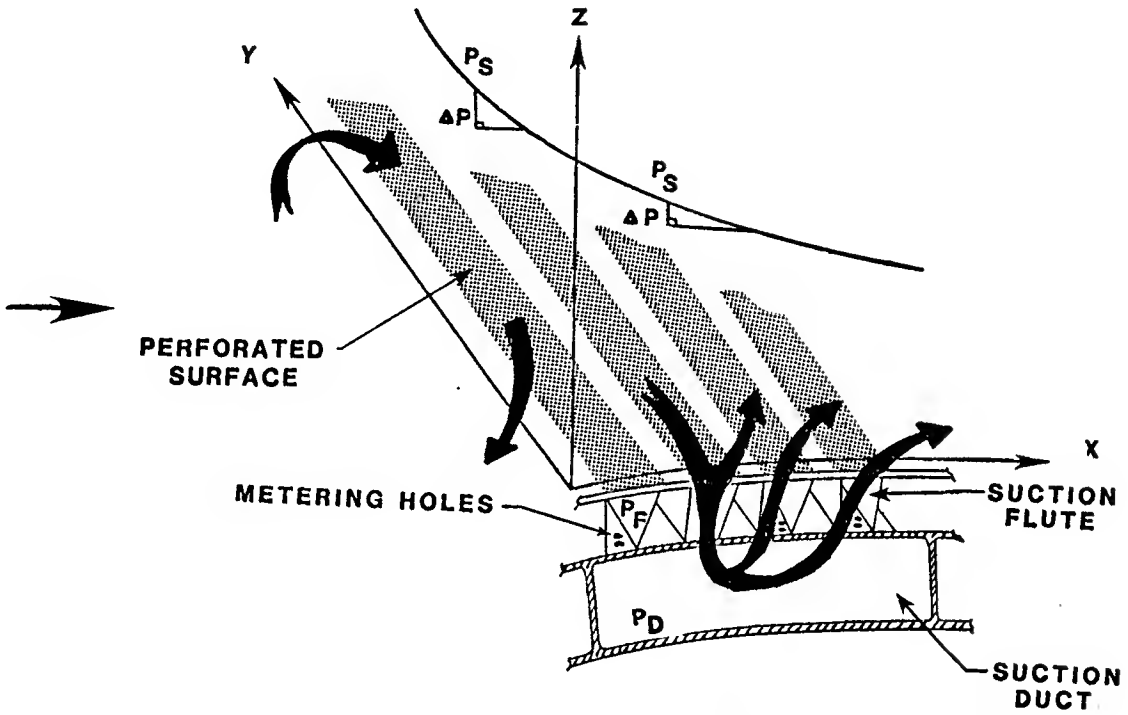

DESIGN PARAMETER	SPANWISE ΔP	CHORDWISE ΔP
METERING HOLES	X	X
BAFFLE DAM	X	
OVERSUCTION	X	X
EBP HOLE SPACING/SIZE	X	X

Figure 6. Perforated surface safeguards against outflow.

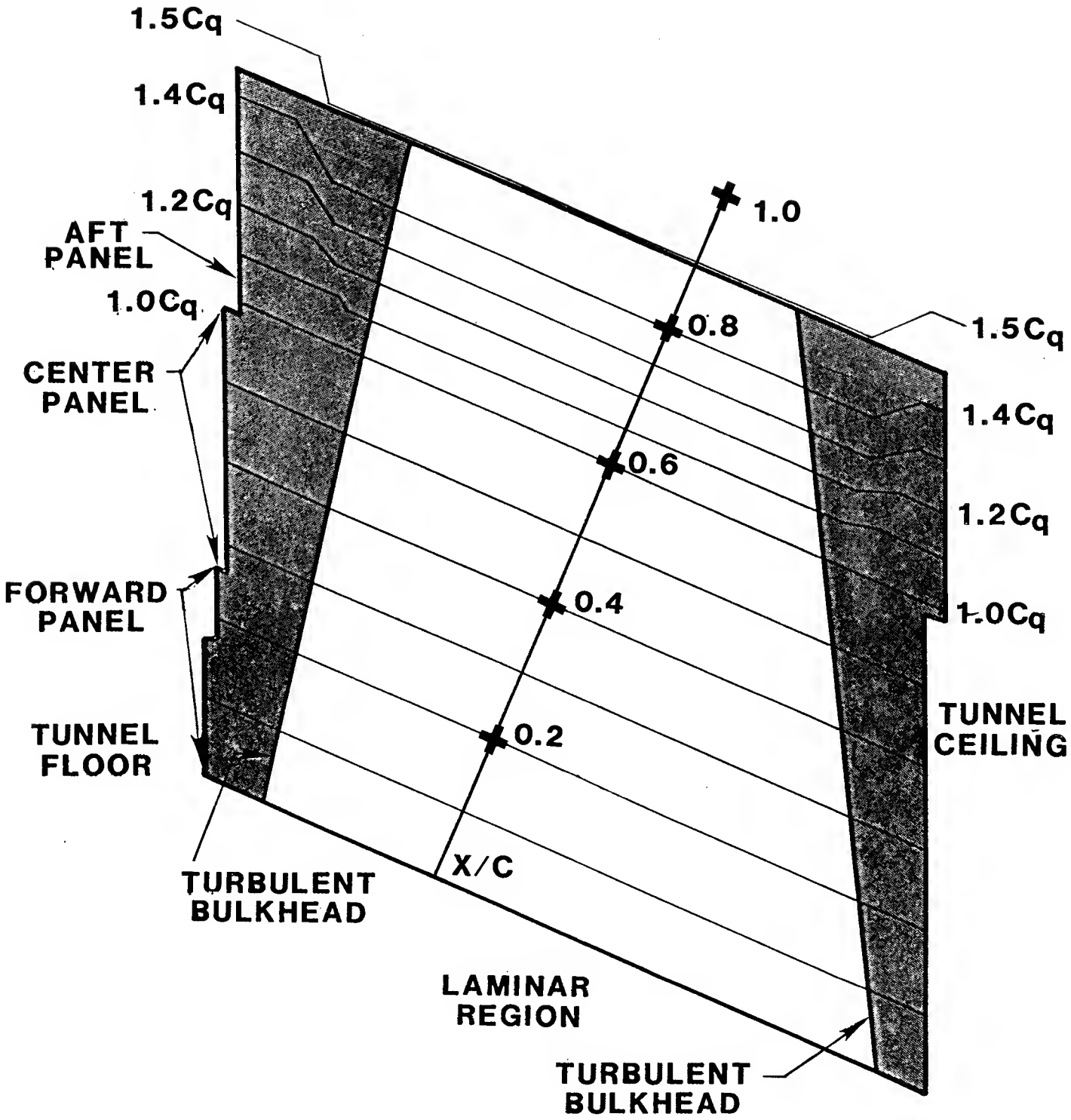

Figure 7. Upper surface suction distribution.

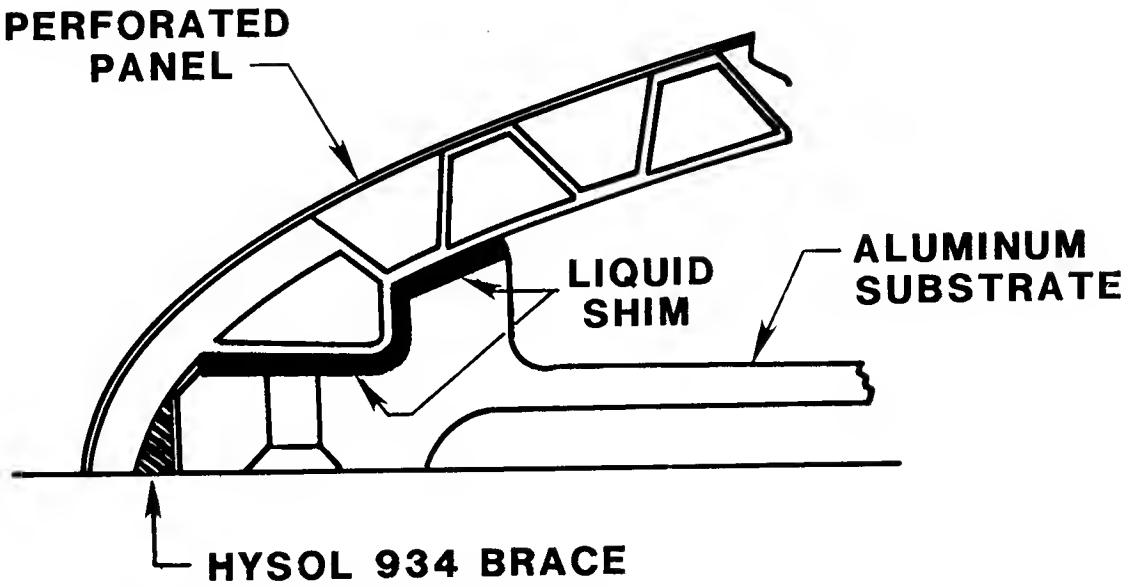

Figure 8. Leading edge design.

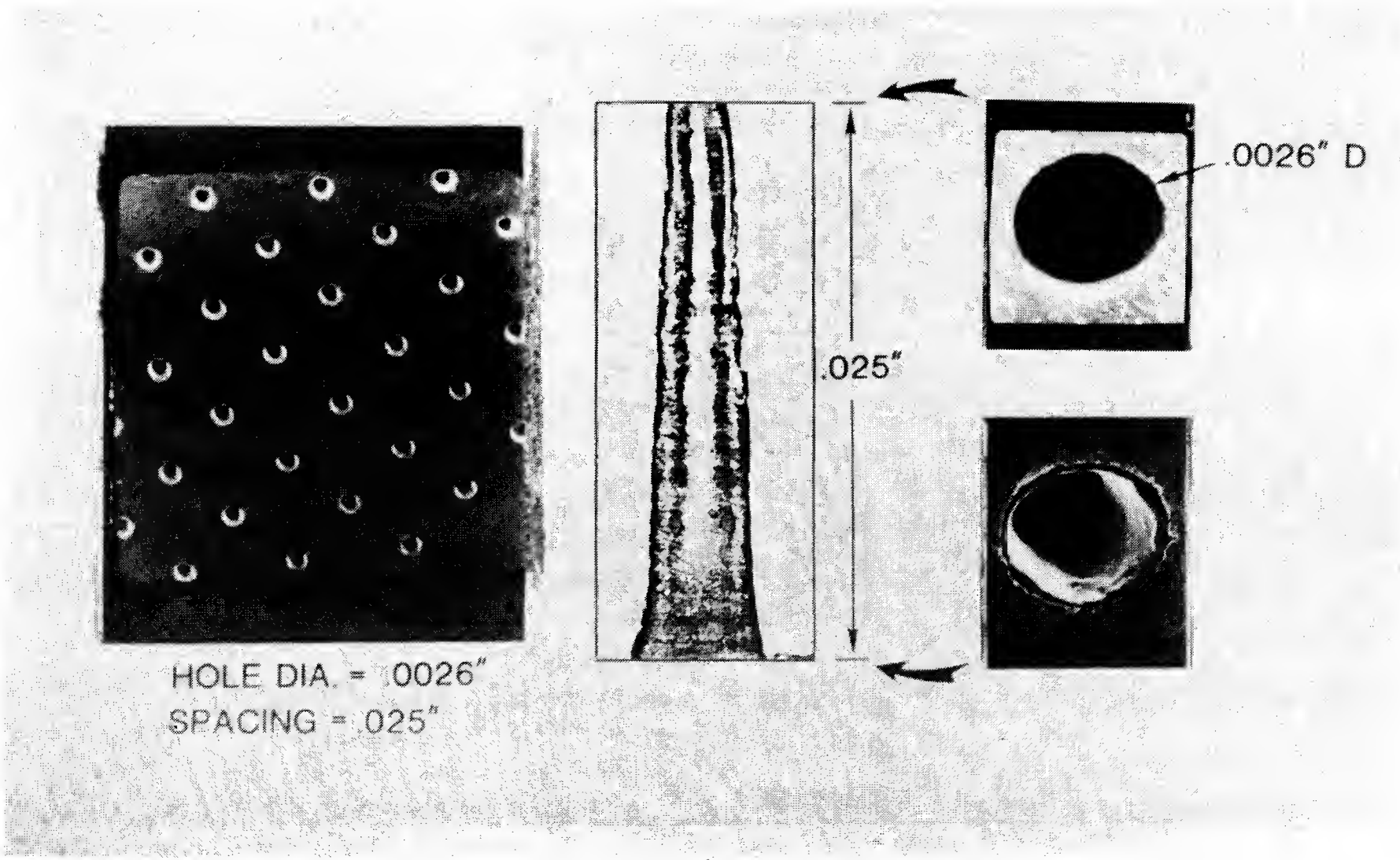

Figure 9. Electron beam perforated titanium.

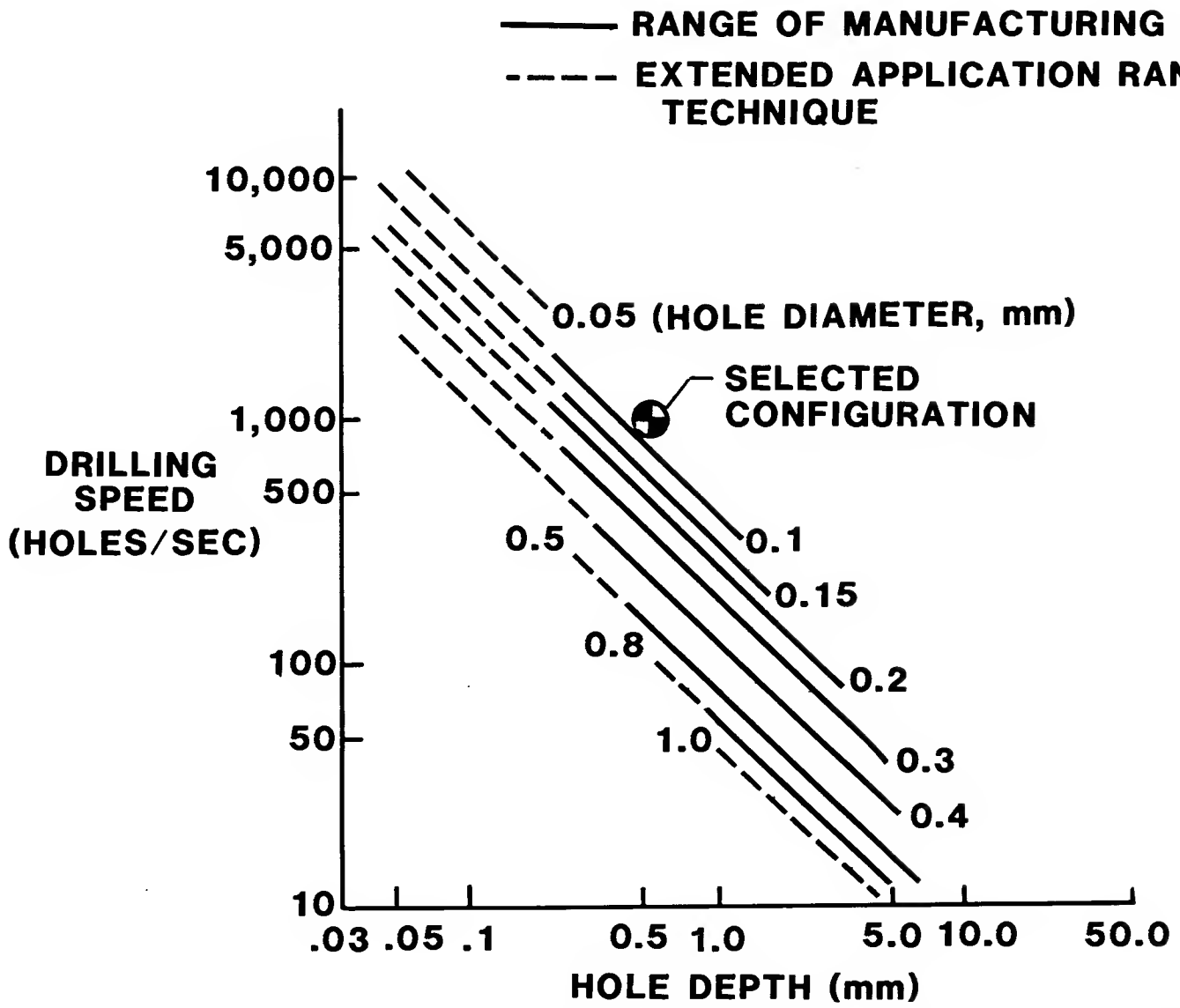

Figure 10. Perforated titanium drilling speeds.

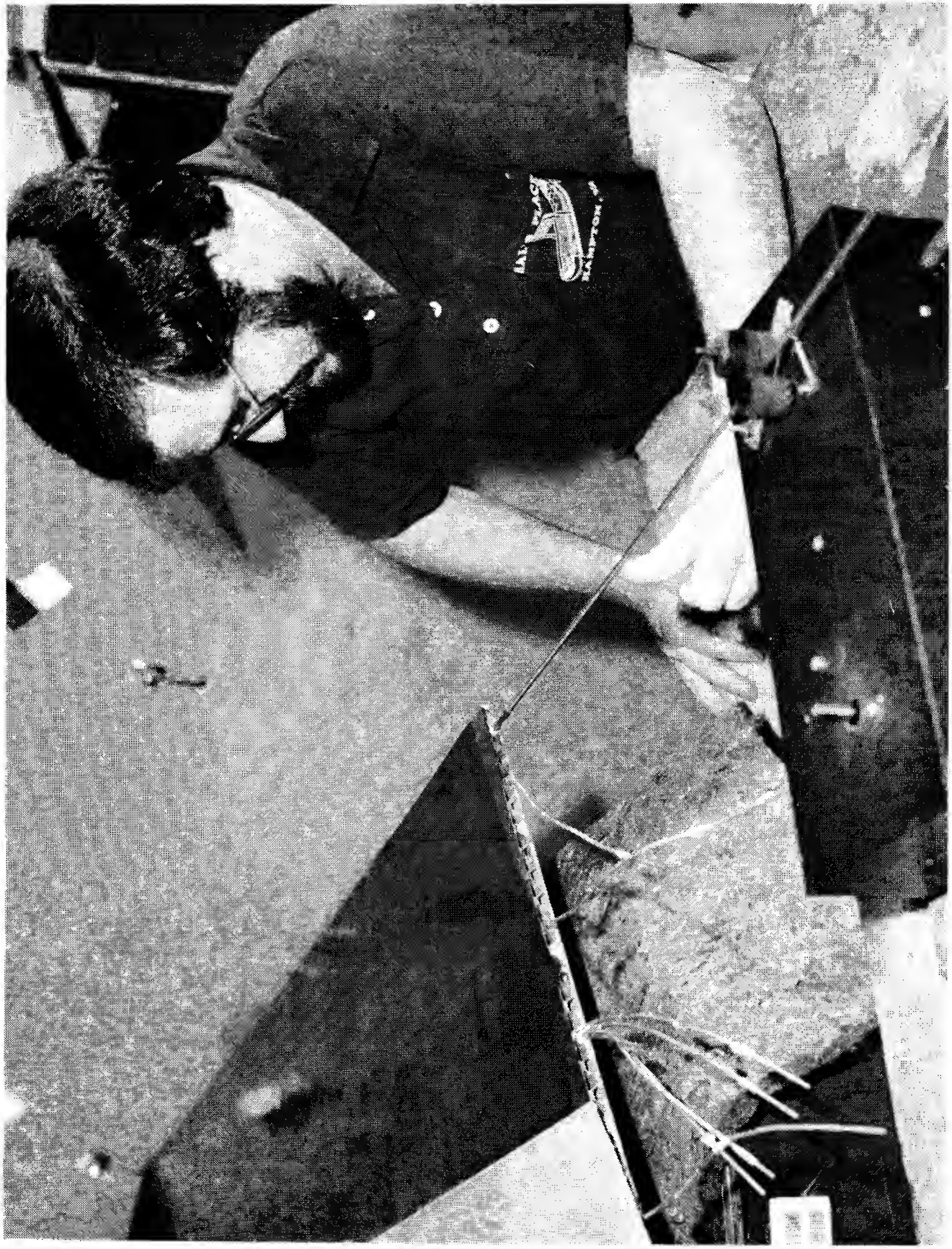

Figure 11. Porosity recording technique.

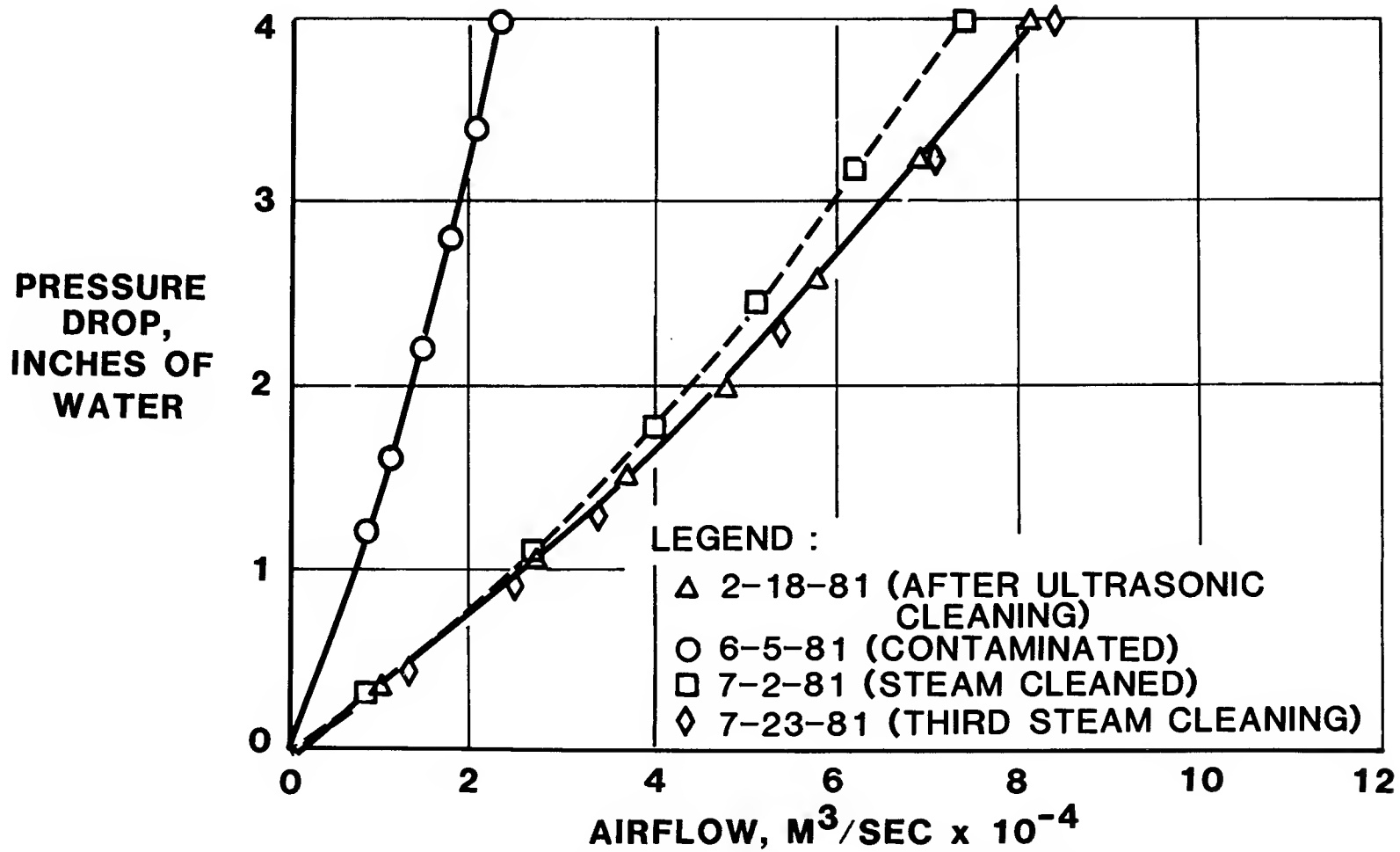

Figure 12. Electron-beam perforated titanium cleaning technique.

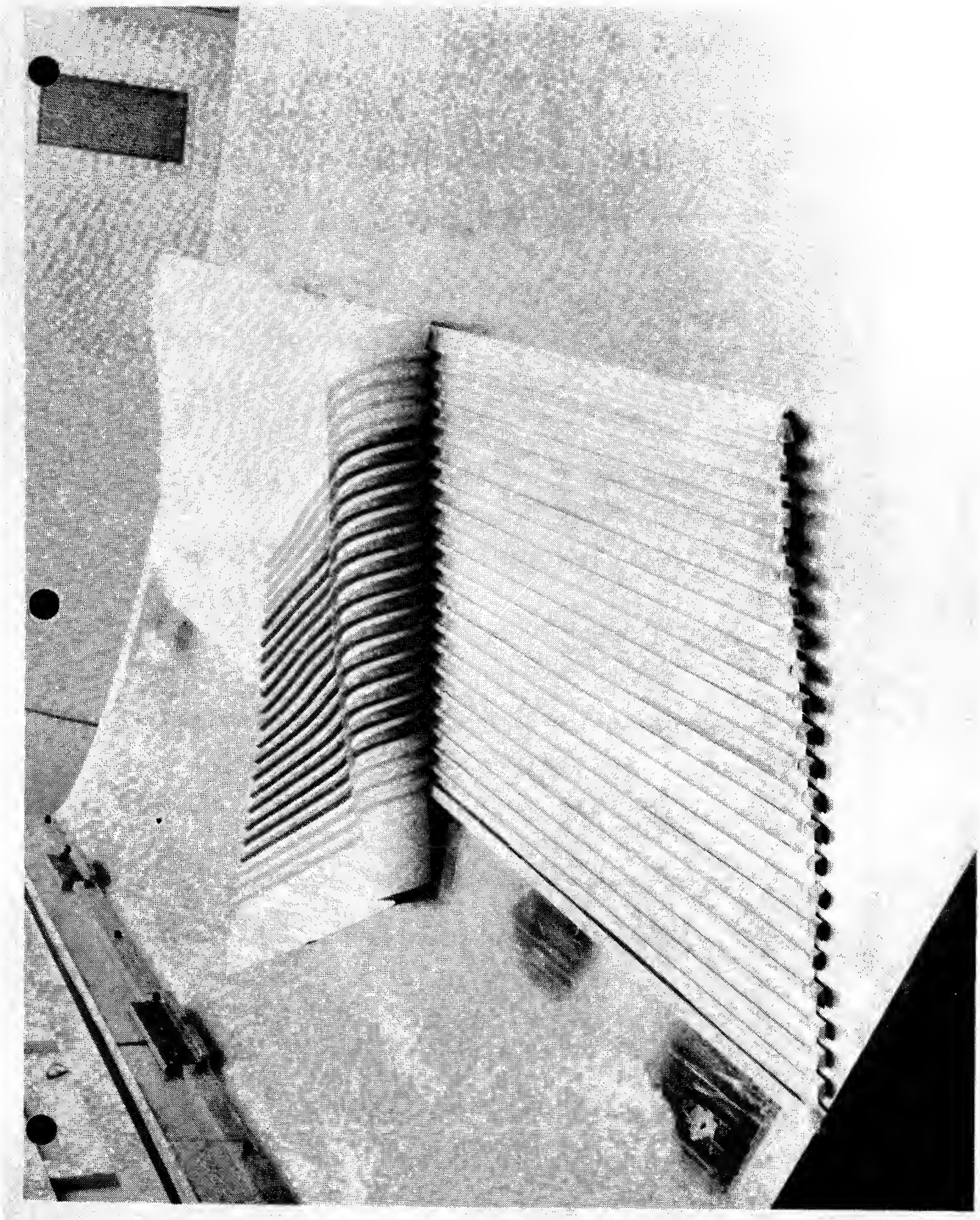

Figure 13. Silcone mandrel layup.

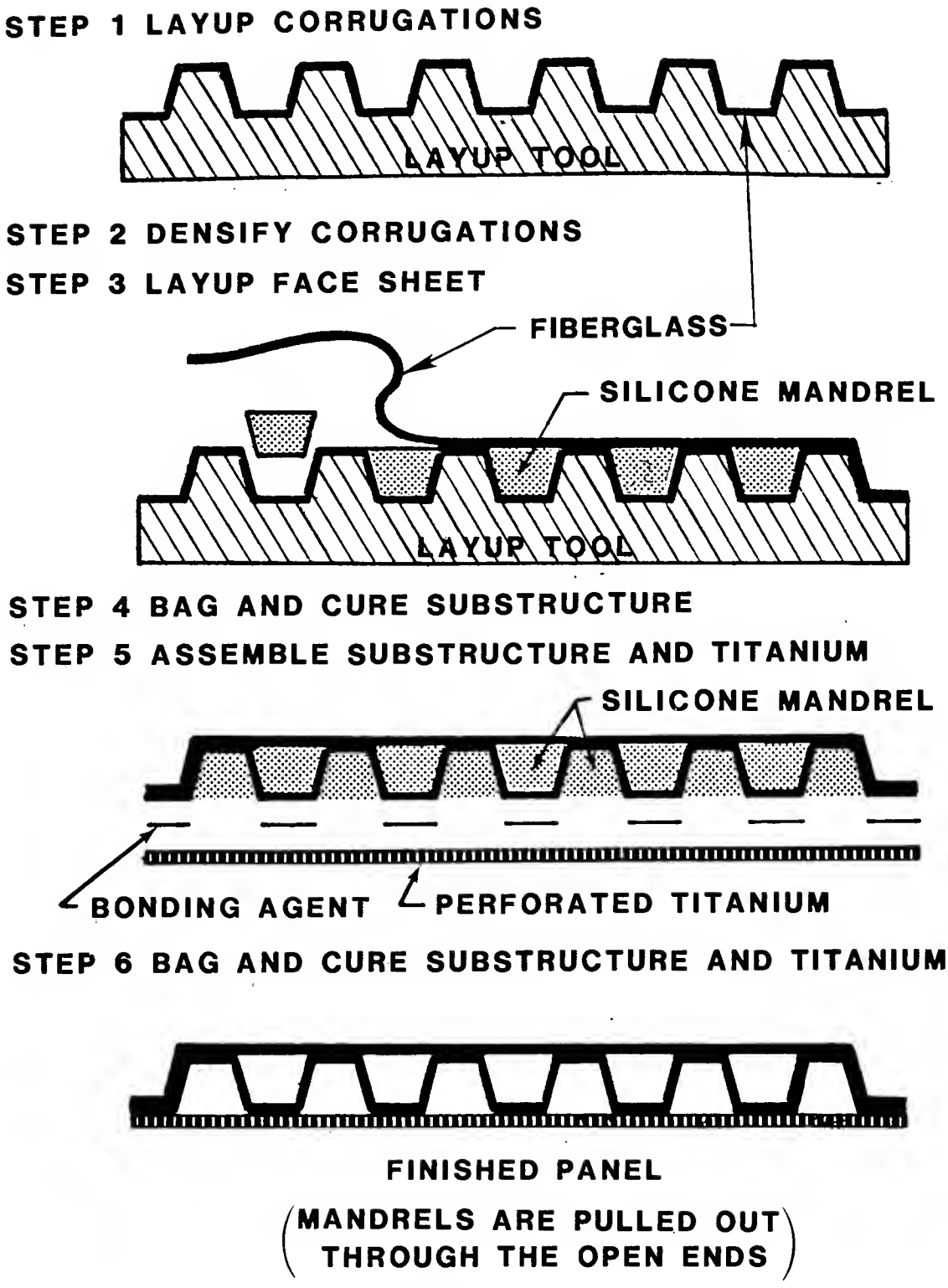

Figure 14. Panel fabrication process.

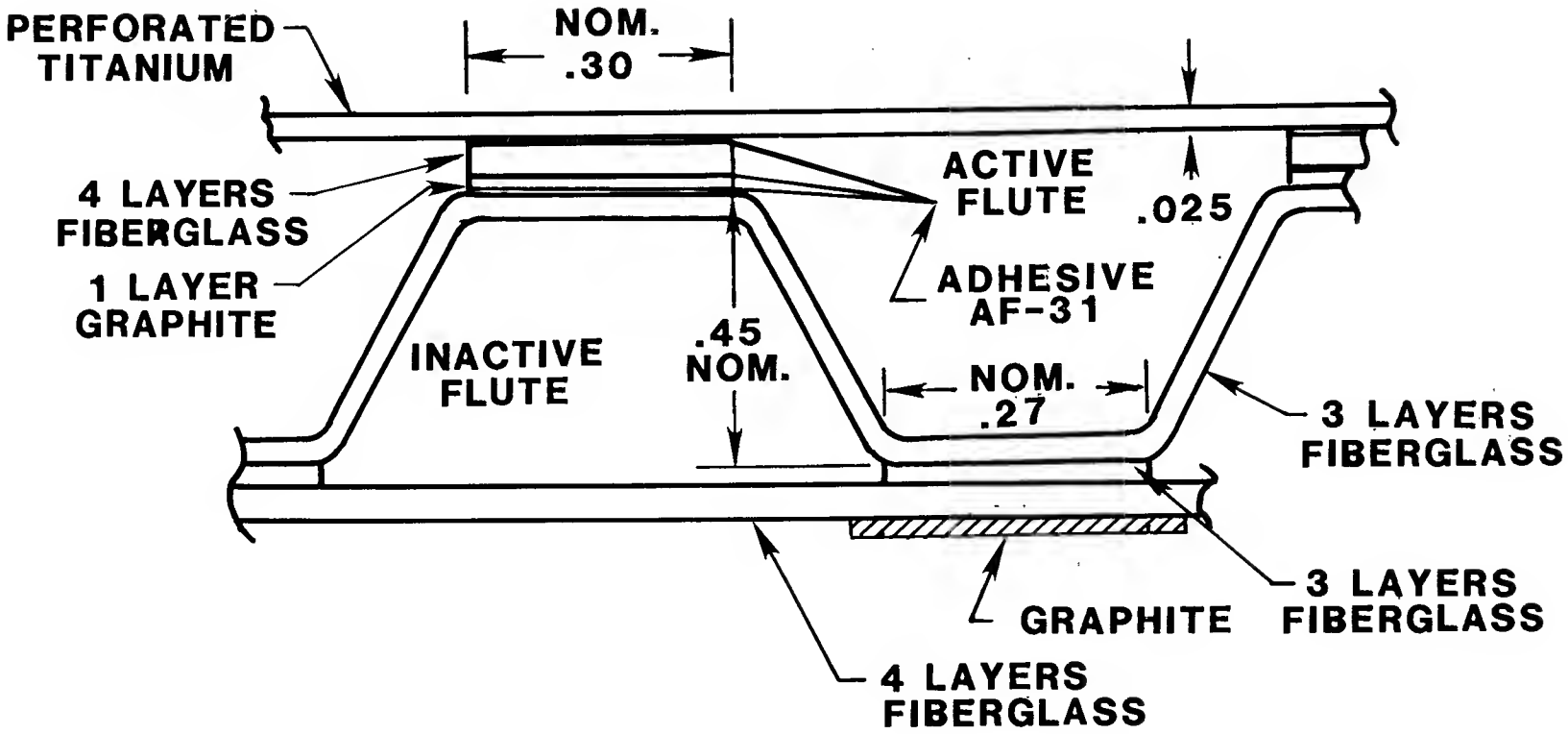

Figure 15. Flute design.

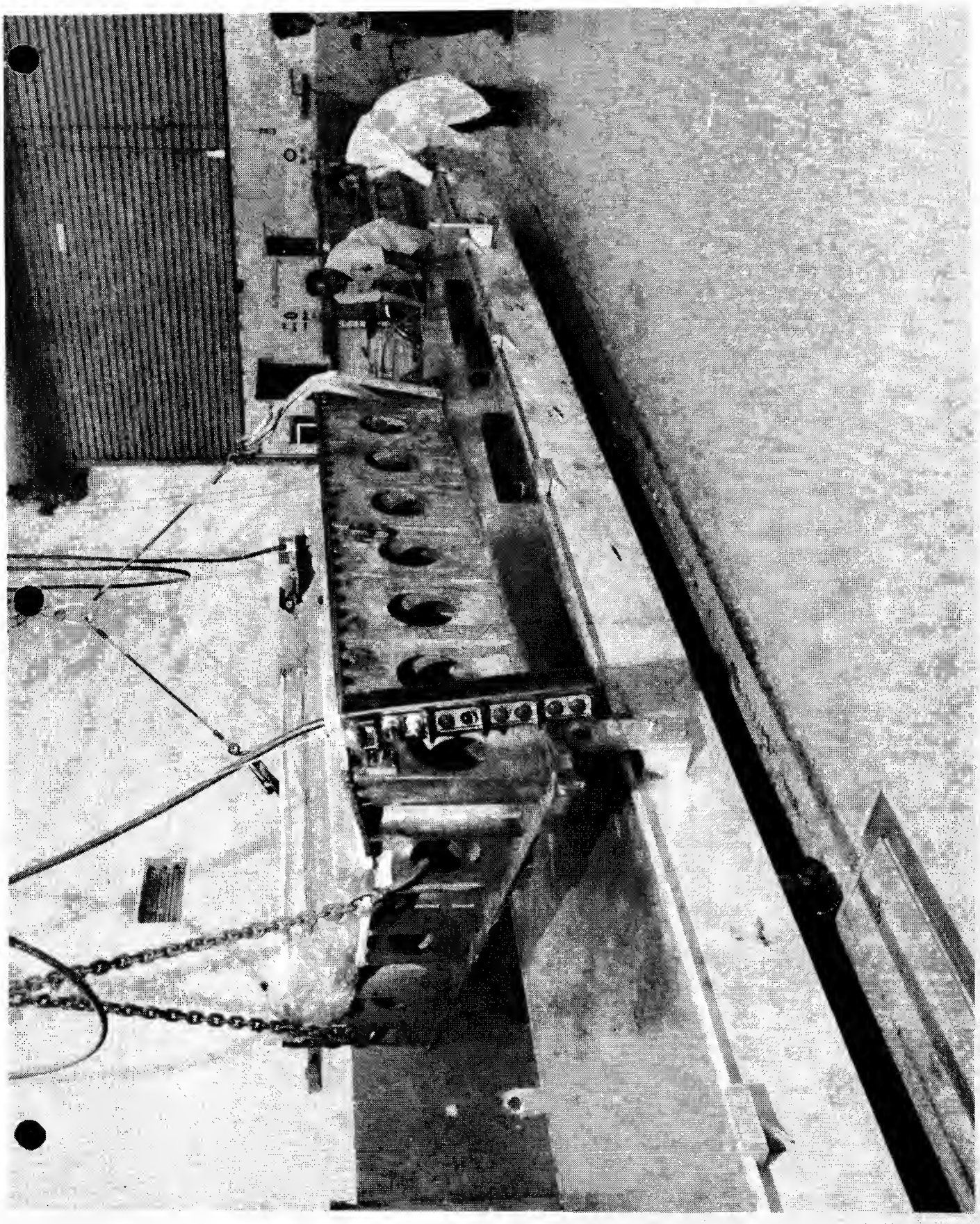

Figure 16. Electron-beam perforated panels on master tool.

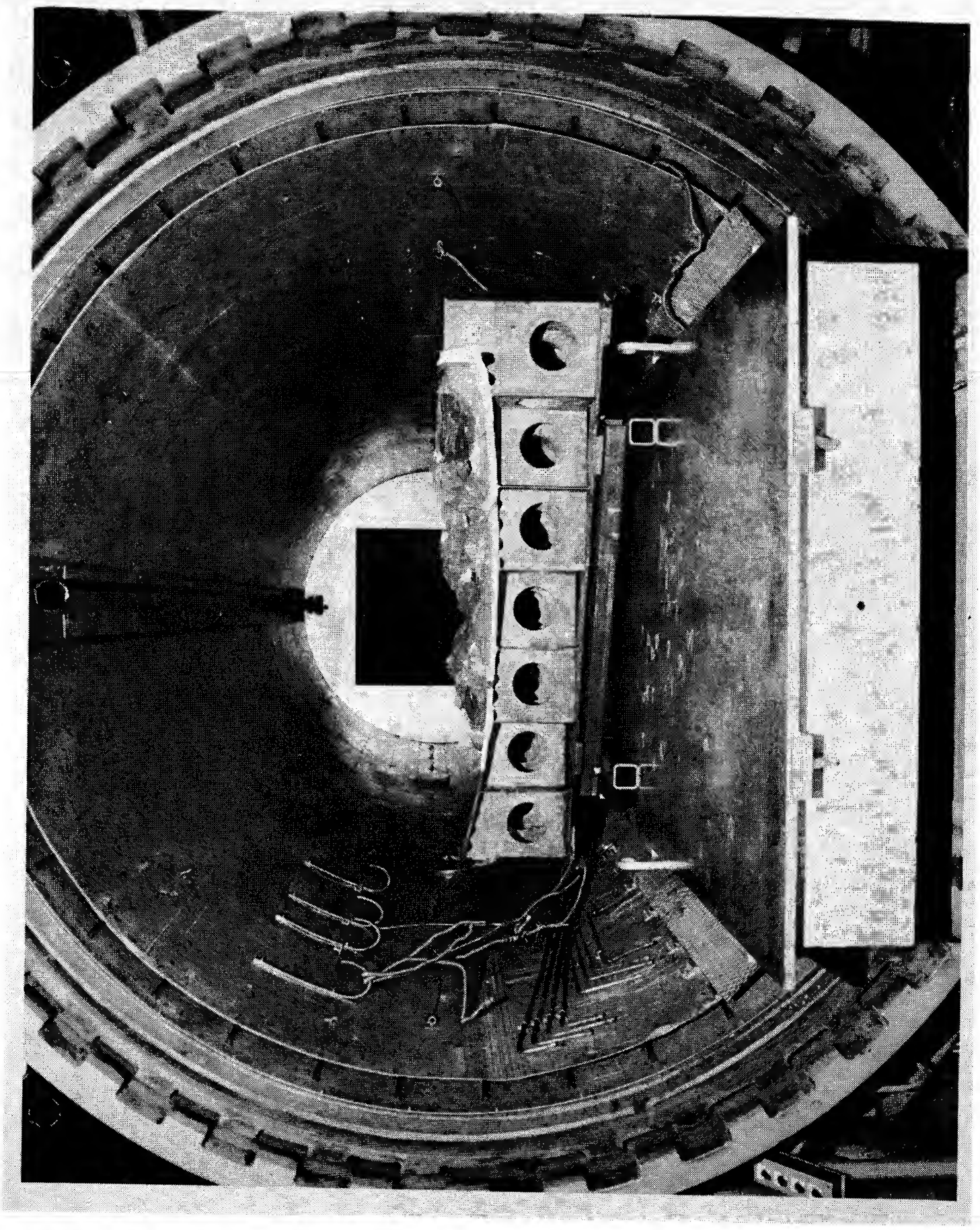

Figure 17. Master tool in autoclave.

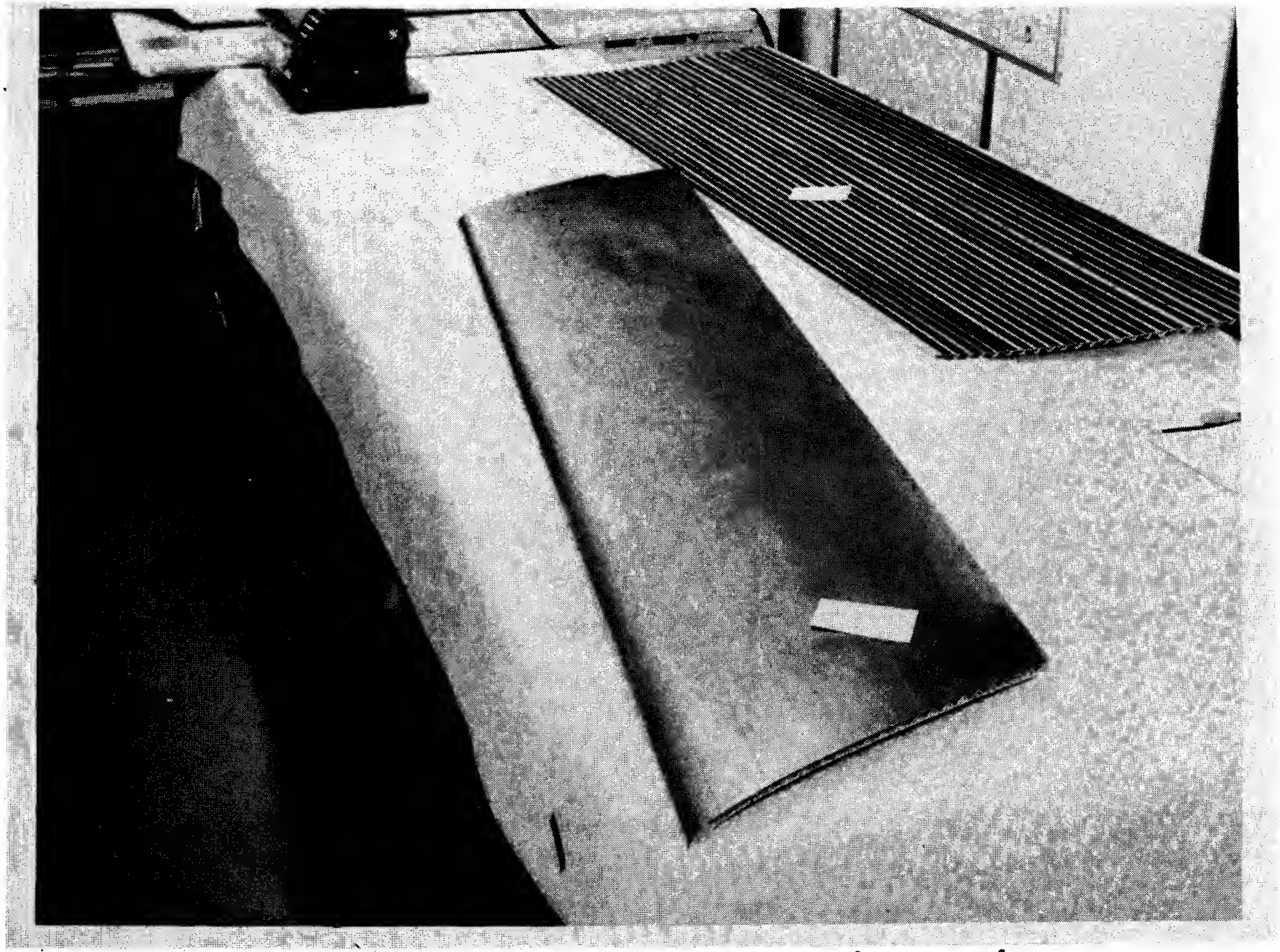

Figure 18. Completed panels, upper and lower surface.

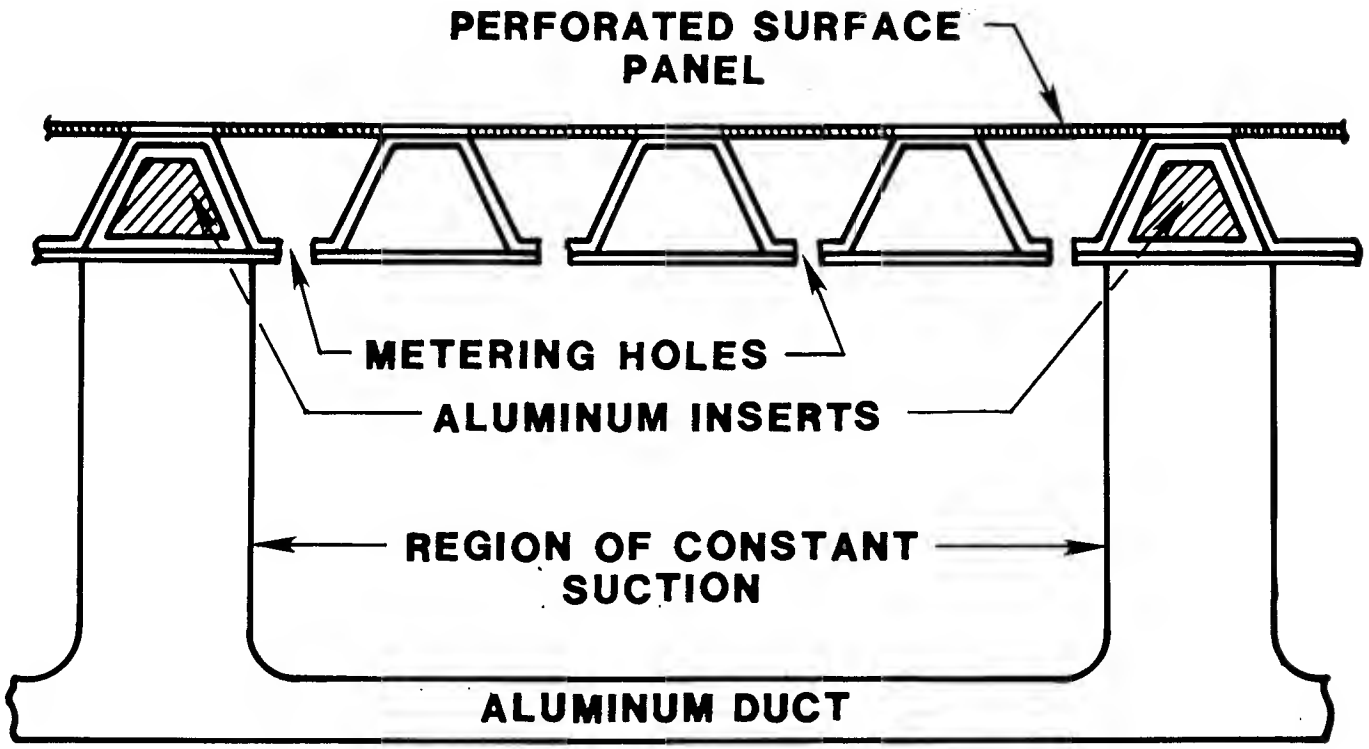

Figure 19. Sketch of skin-flute-duct design.

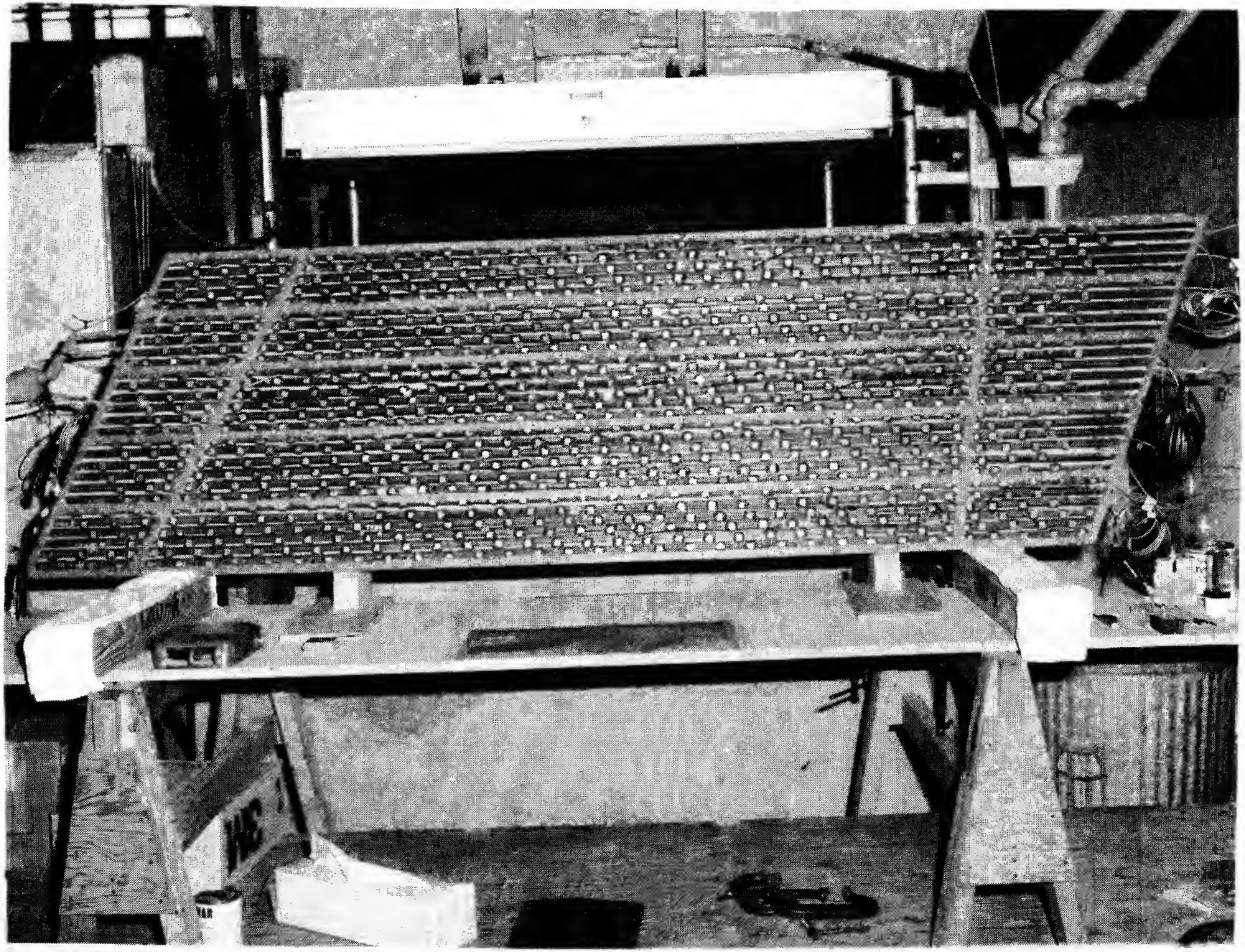

Figure 20. Completed panel backside.

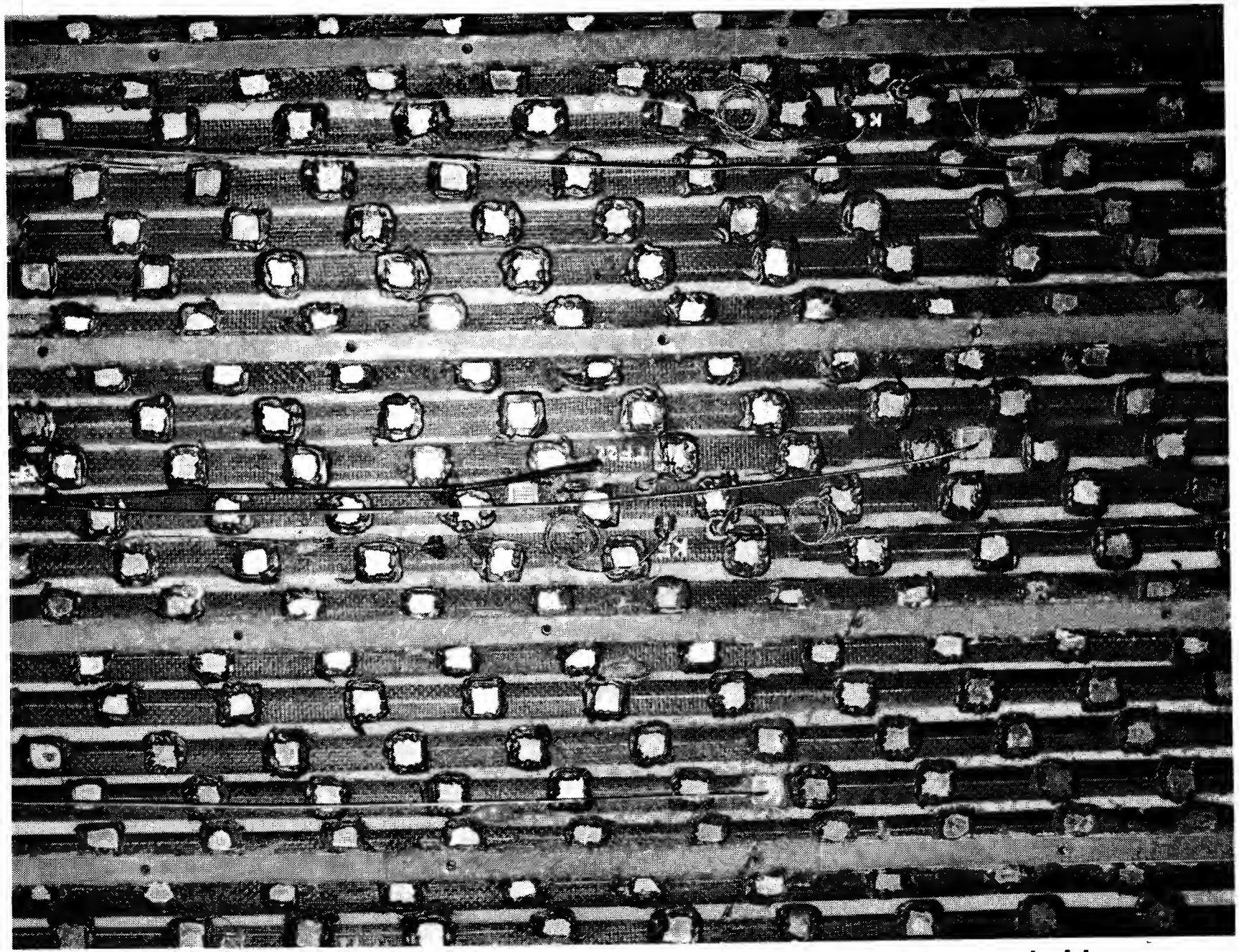

Figure 21. Aluminum metering hole squares on panel backside.

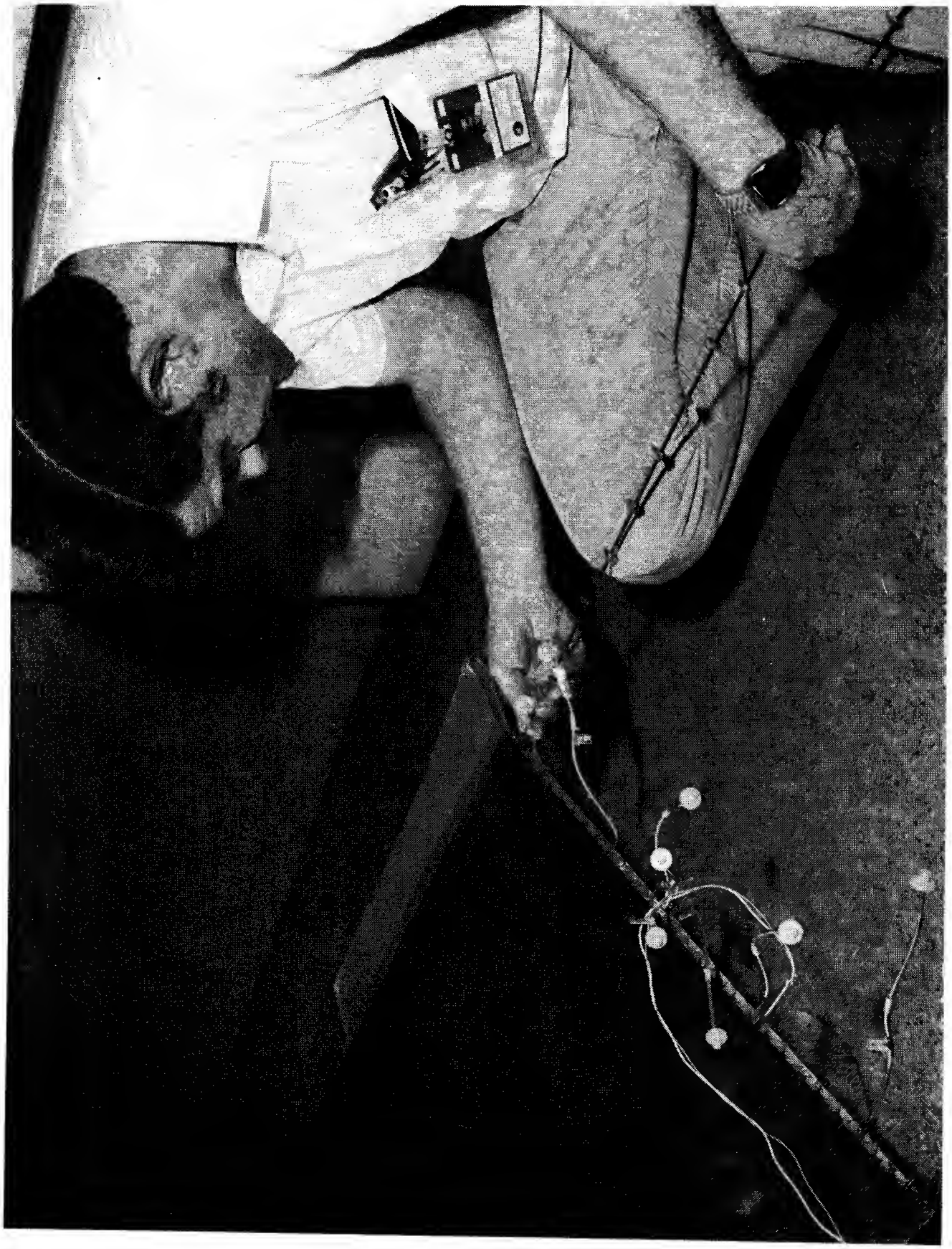

Figure 22. Installation of baffle rods.

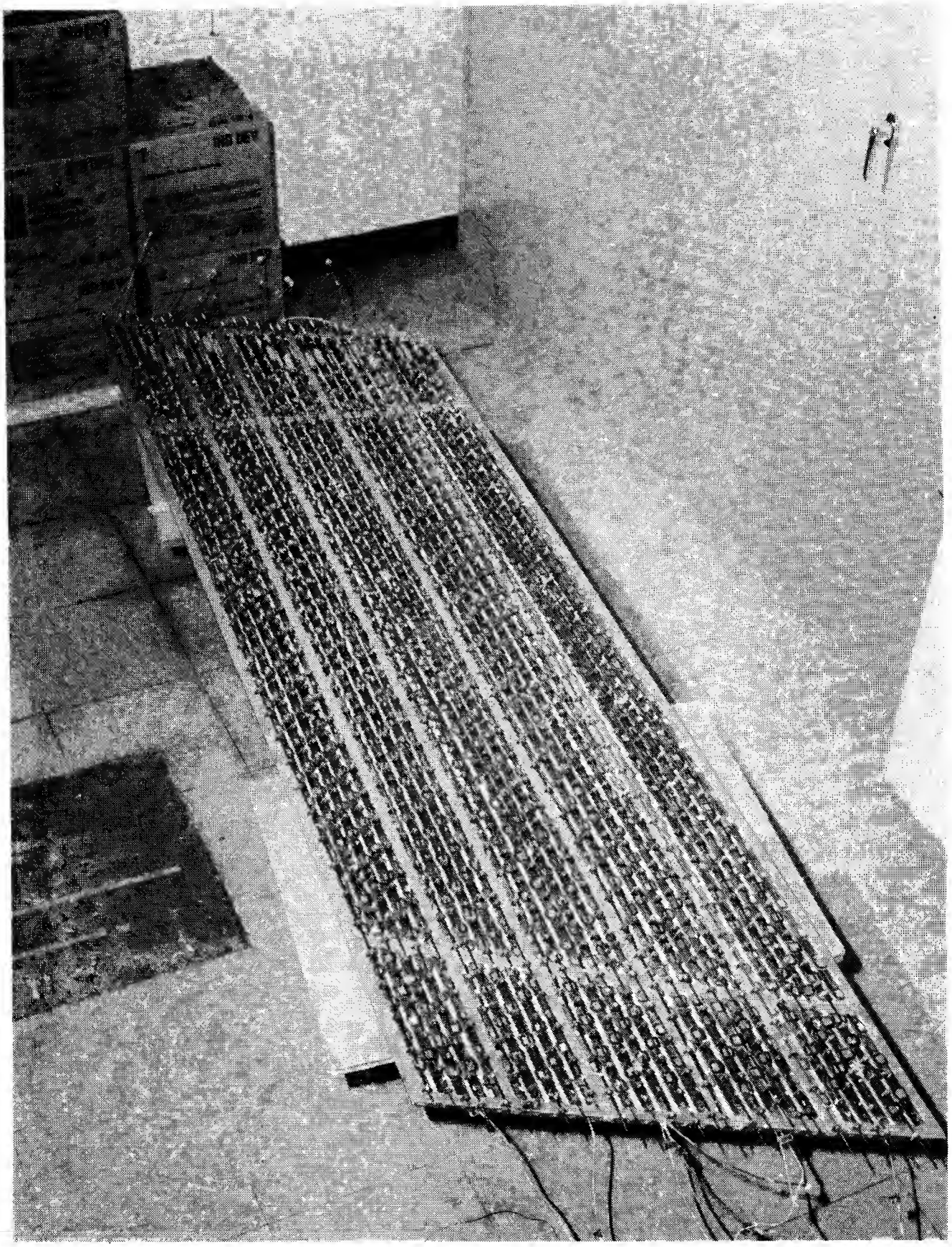

Figure 23. Location of baffle rods.

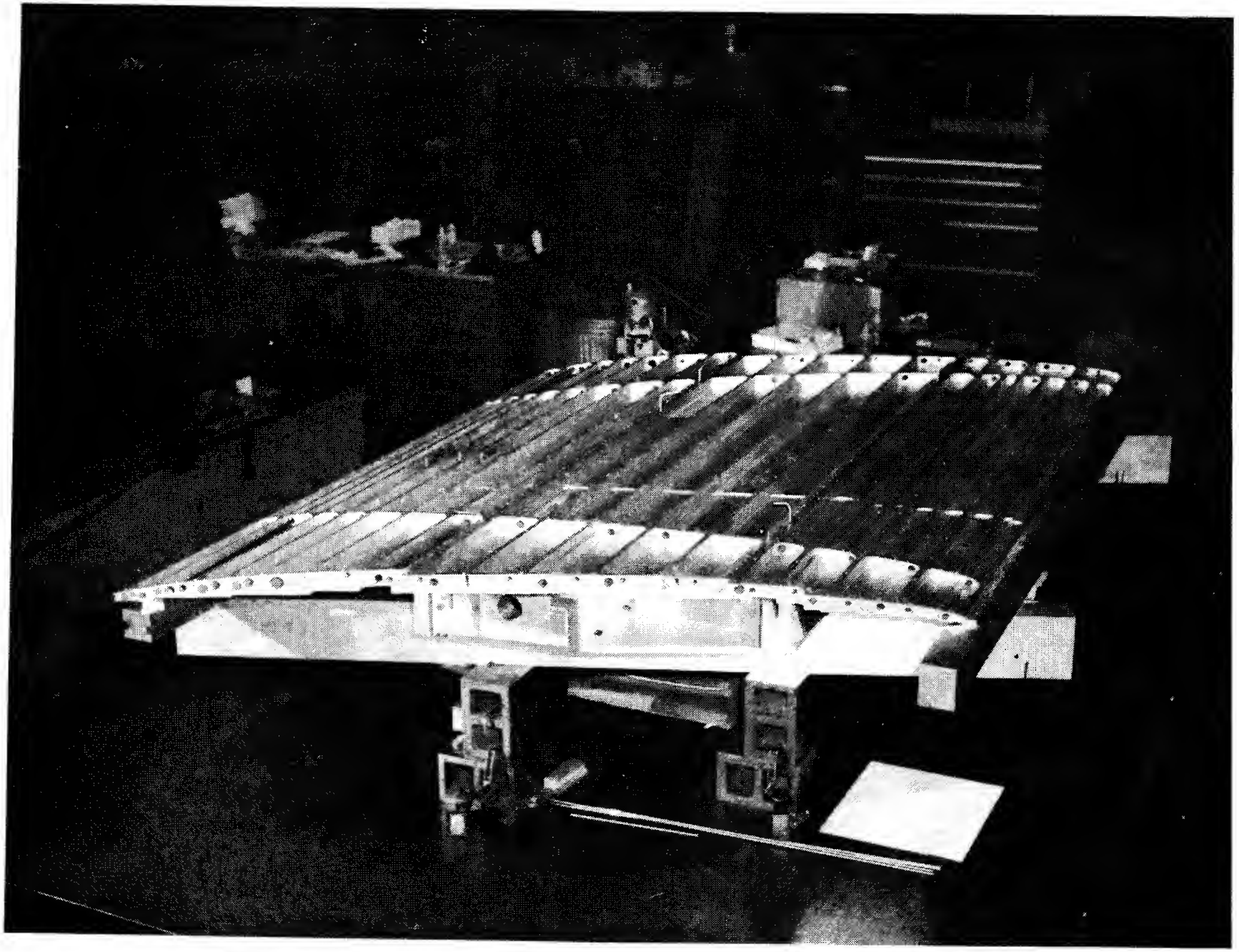

Figure 24. Aluminum ducts mounted on wing box.

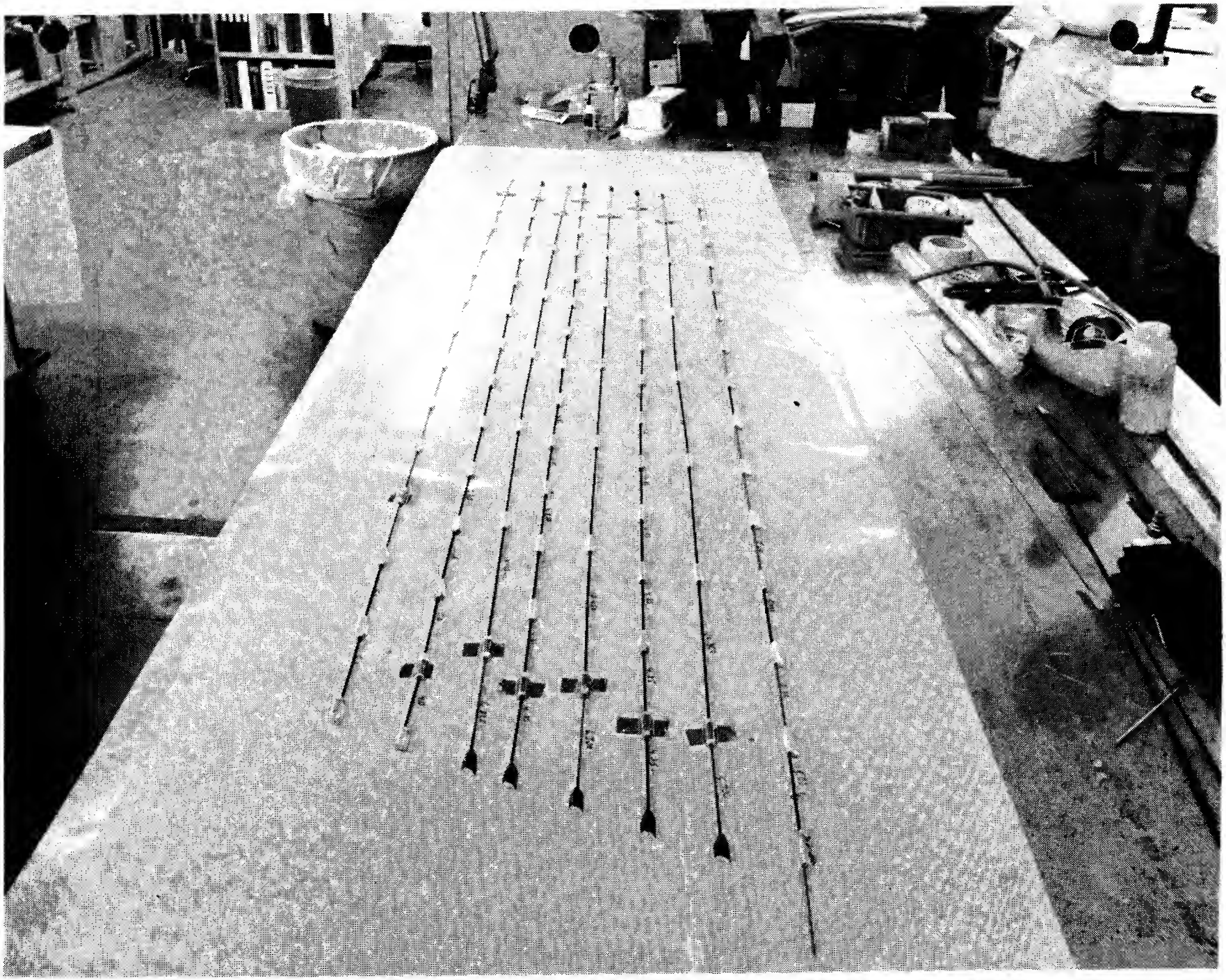

Figure 25. Panel aluminum inserts.

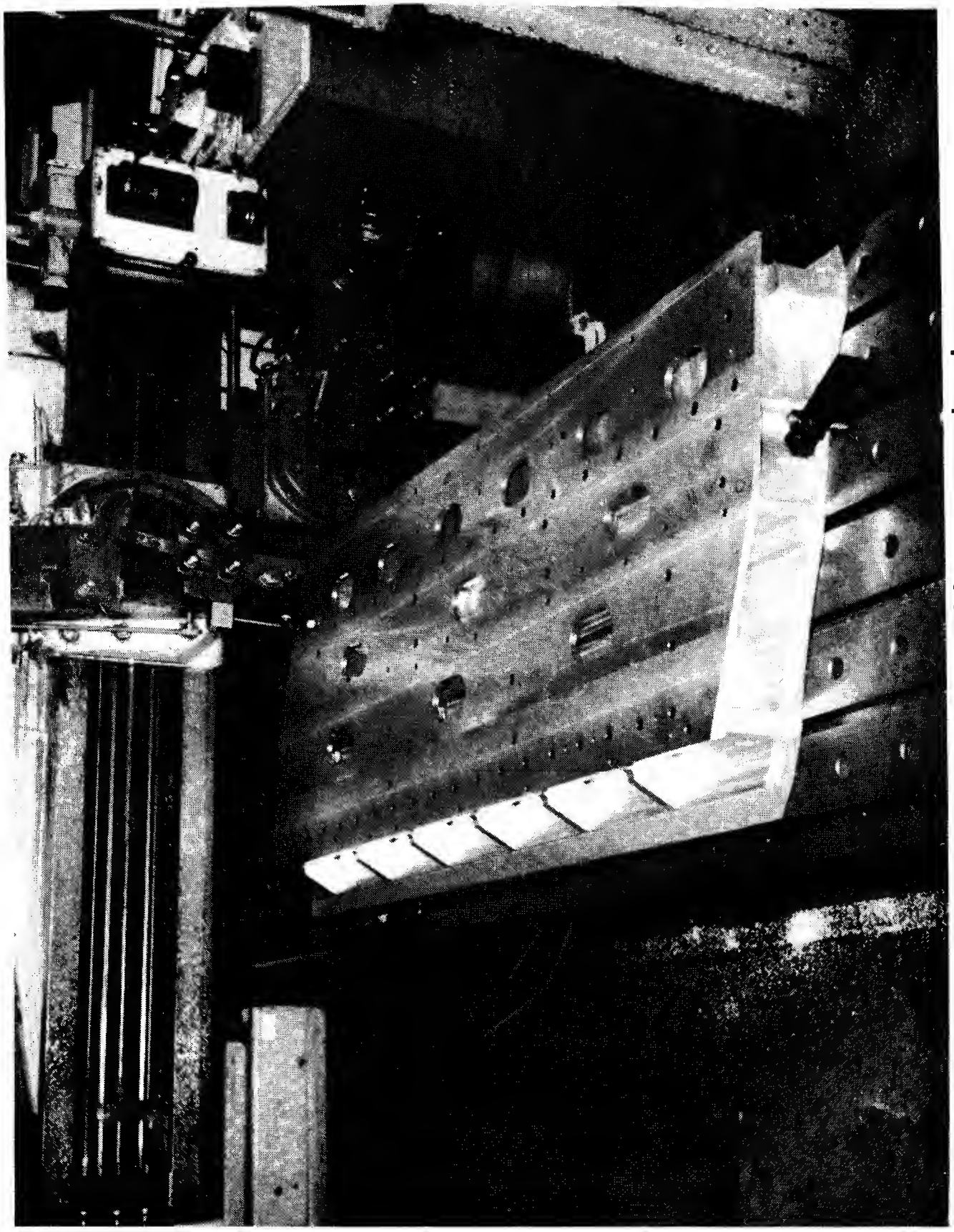

Figure 26. Variable sweep wing box.

Figure 27. Completed electron beam perforated model.

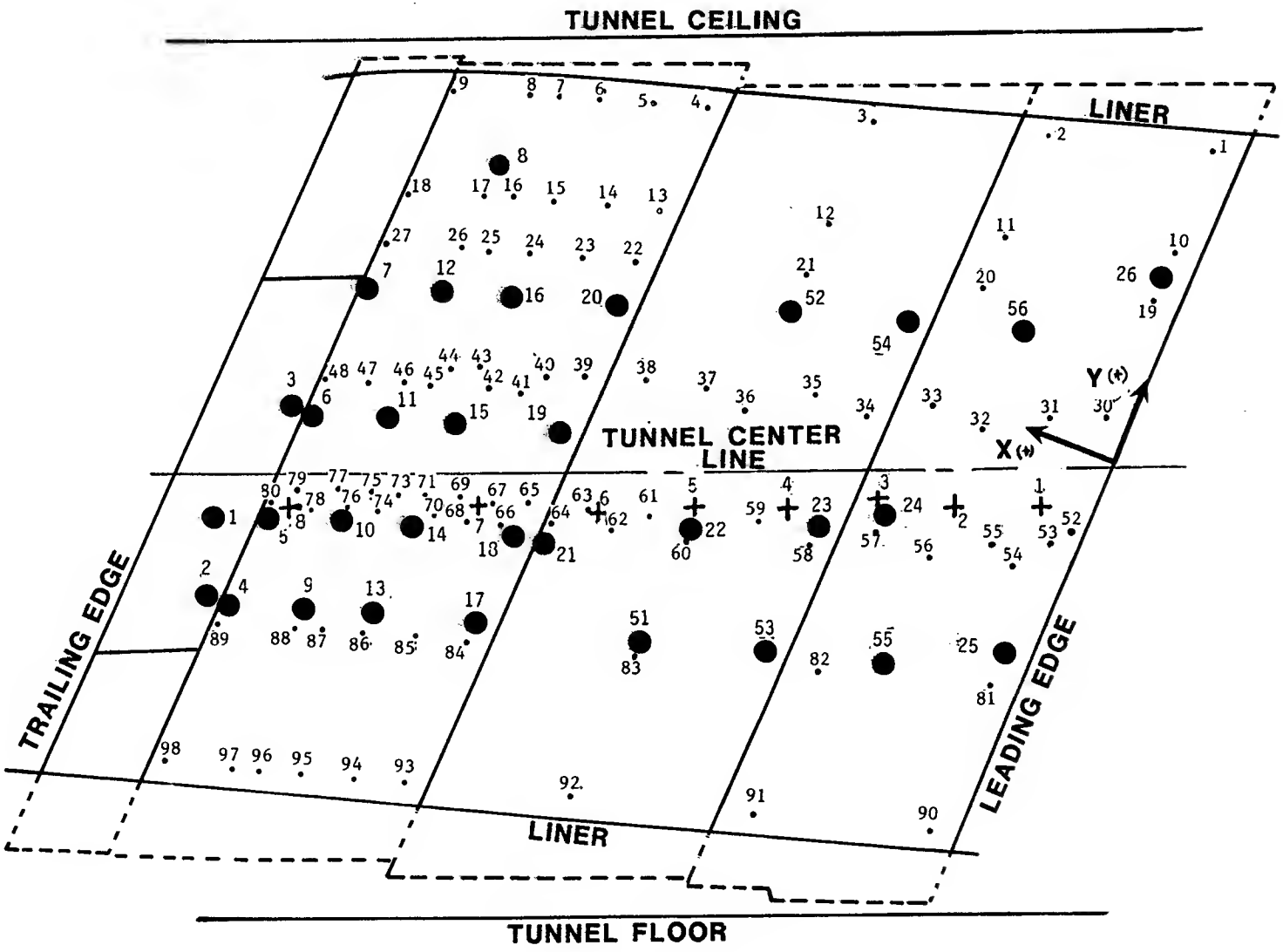

Figure 28. Sketch of airfoil surface instrumentation.

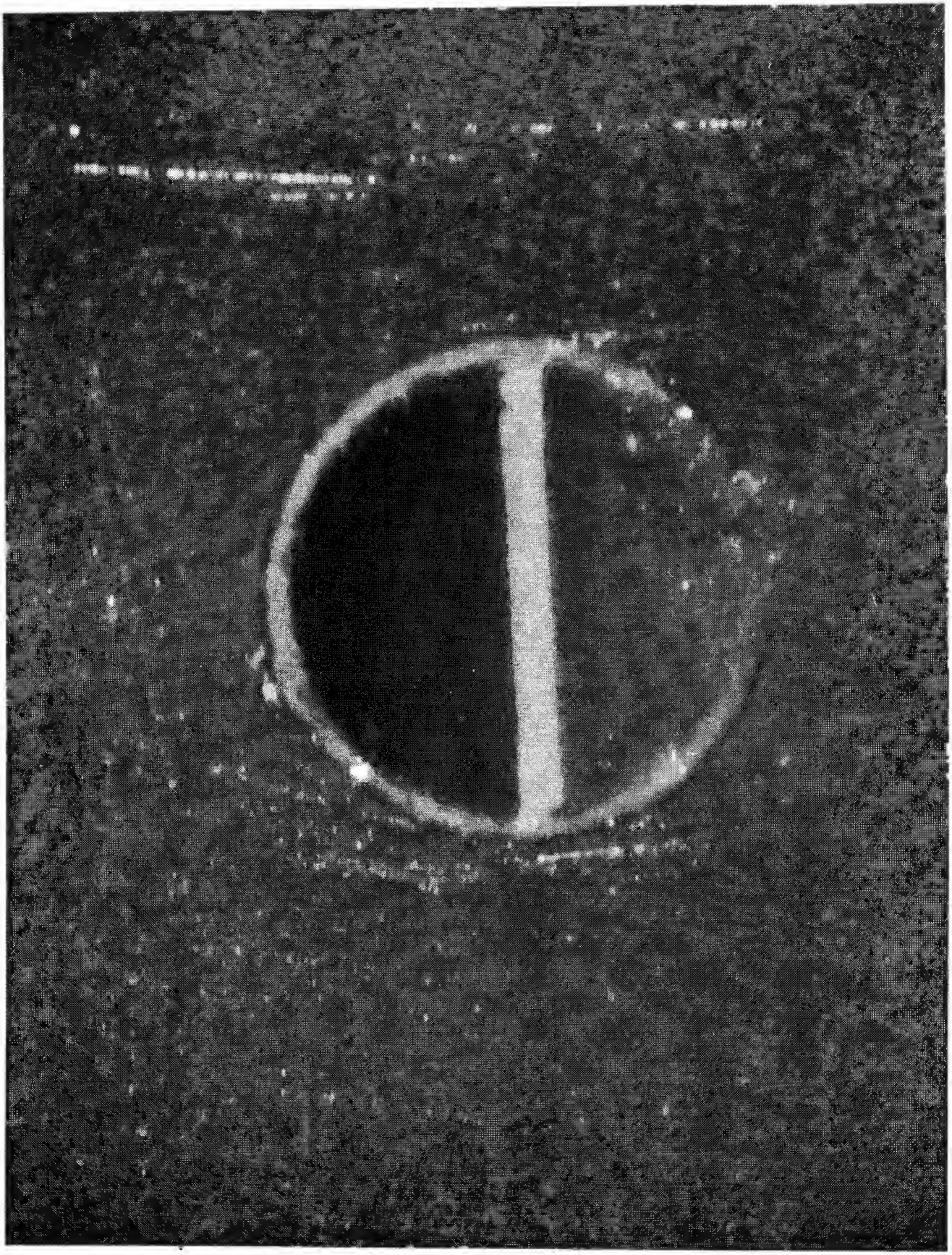

Figure 29. Typical thin film gage surface.

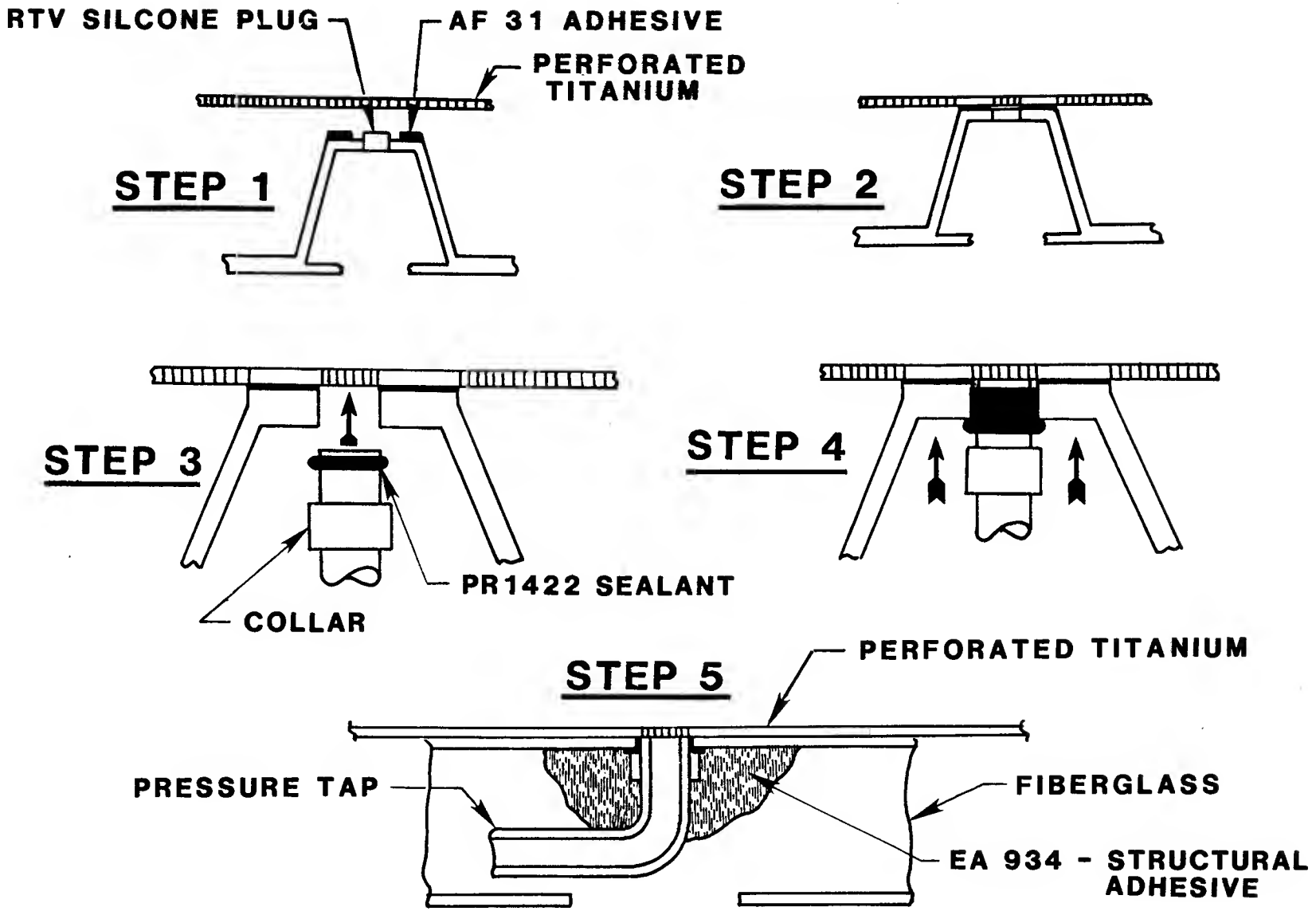

Figure 30. Surface pressure tap installation.

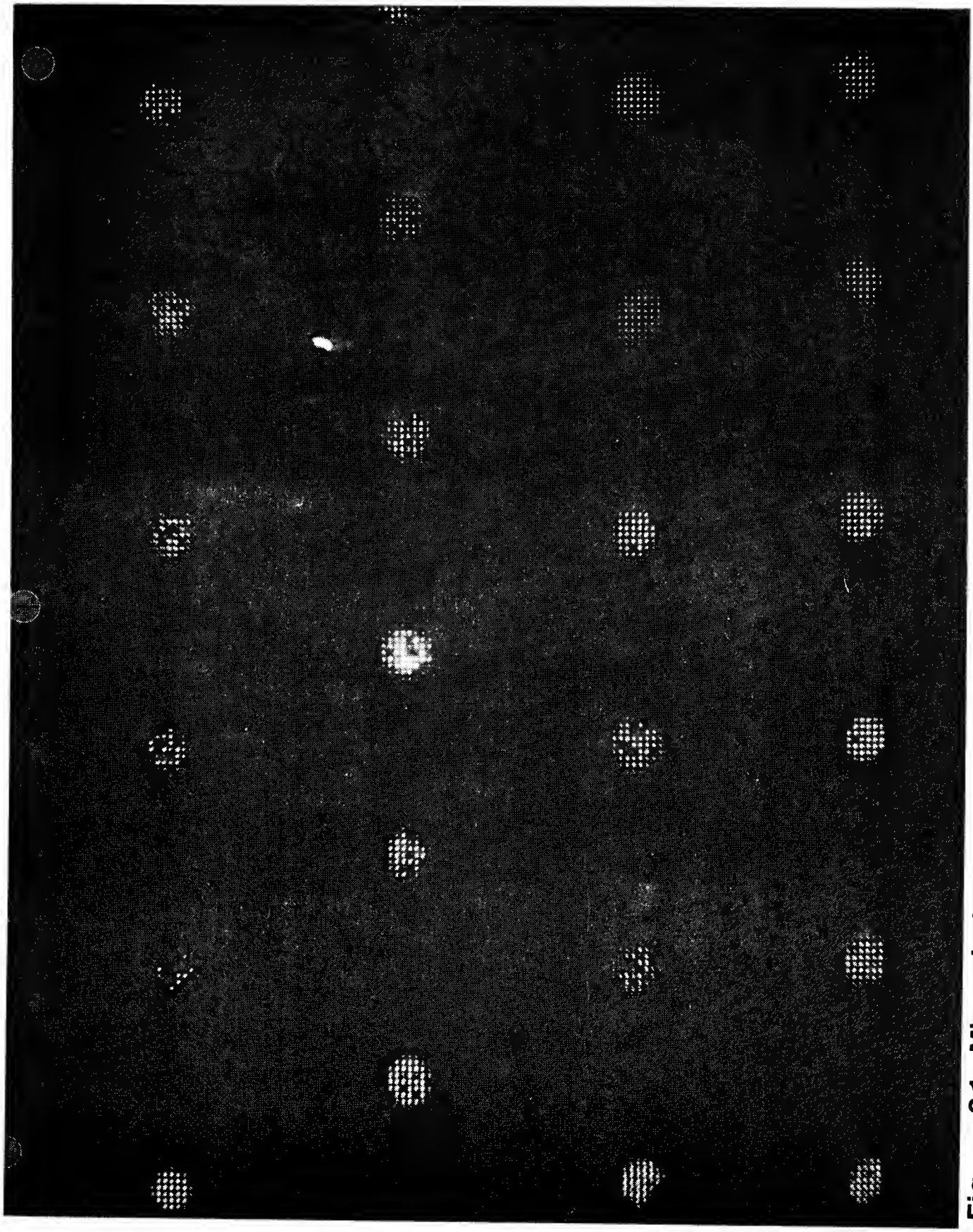

Figure 31. Microphotograph of electron beam perforated holes showing clogging.

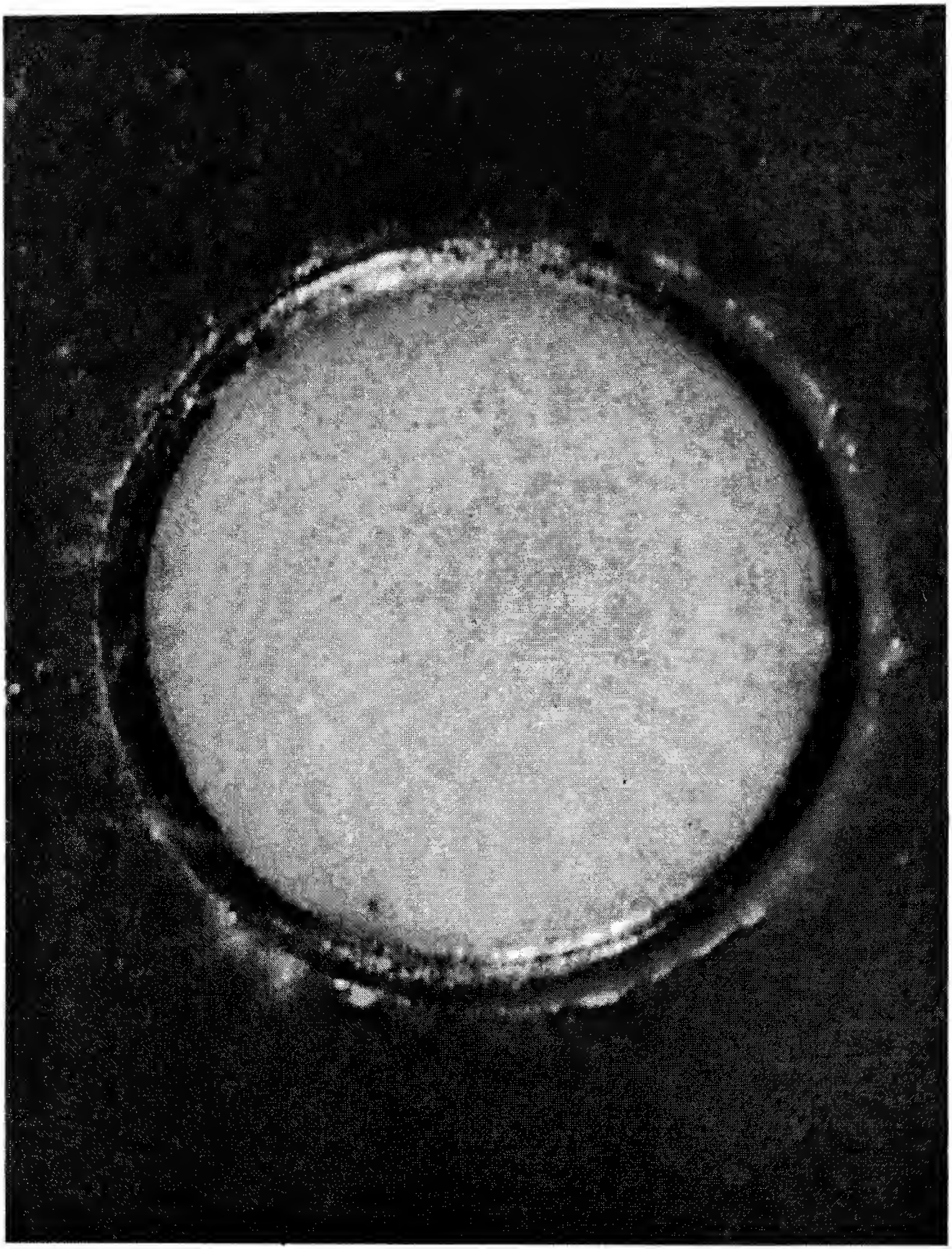

Figure 32. Typical kulite gage surface.

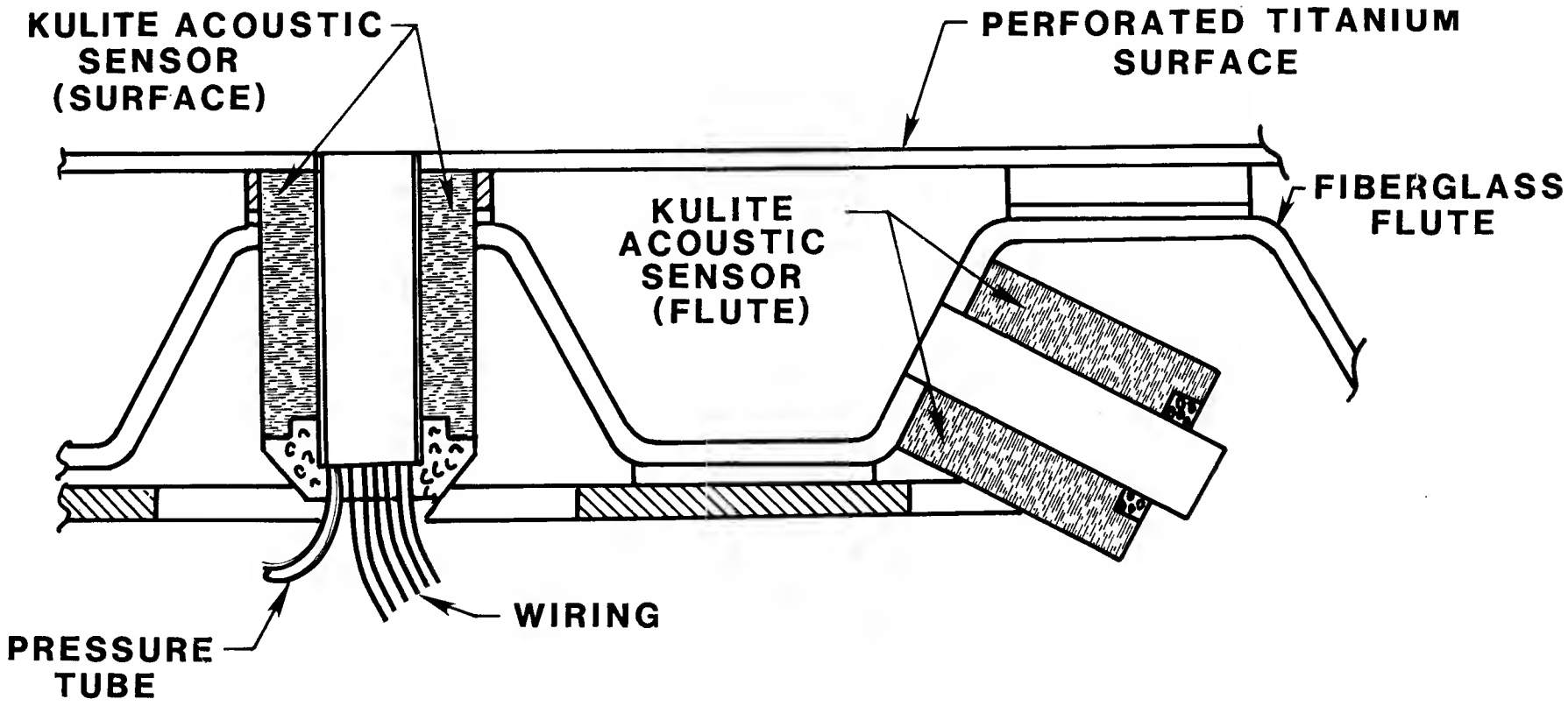

Figure 33. Installation of acoustic instrumentation.

(ALL DIMENSIONS IN INCHES)

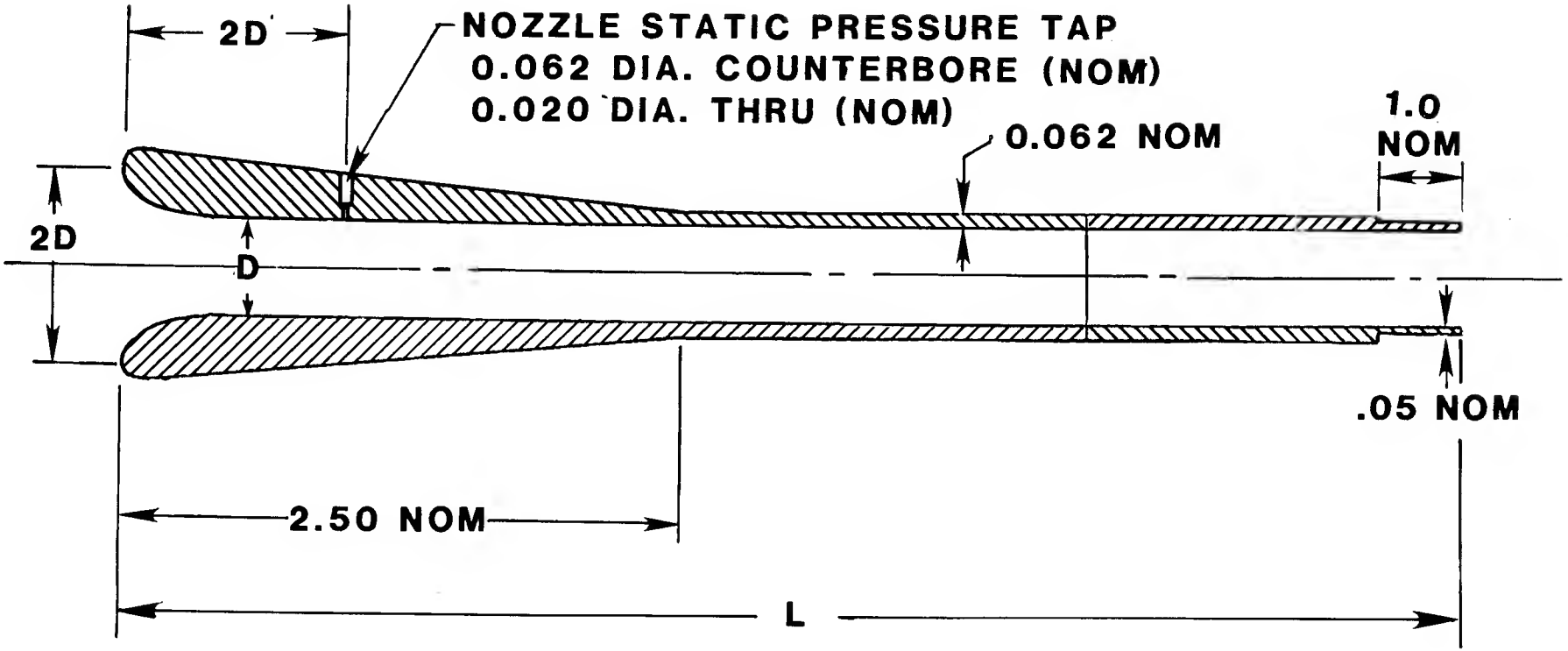

Figure 34. Nozzle configuration.

Figure 35. Nozzles in ducts.

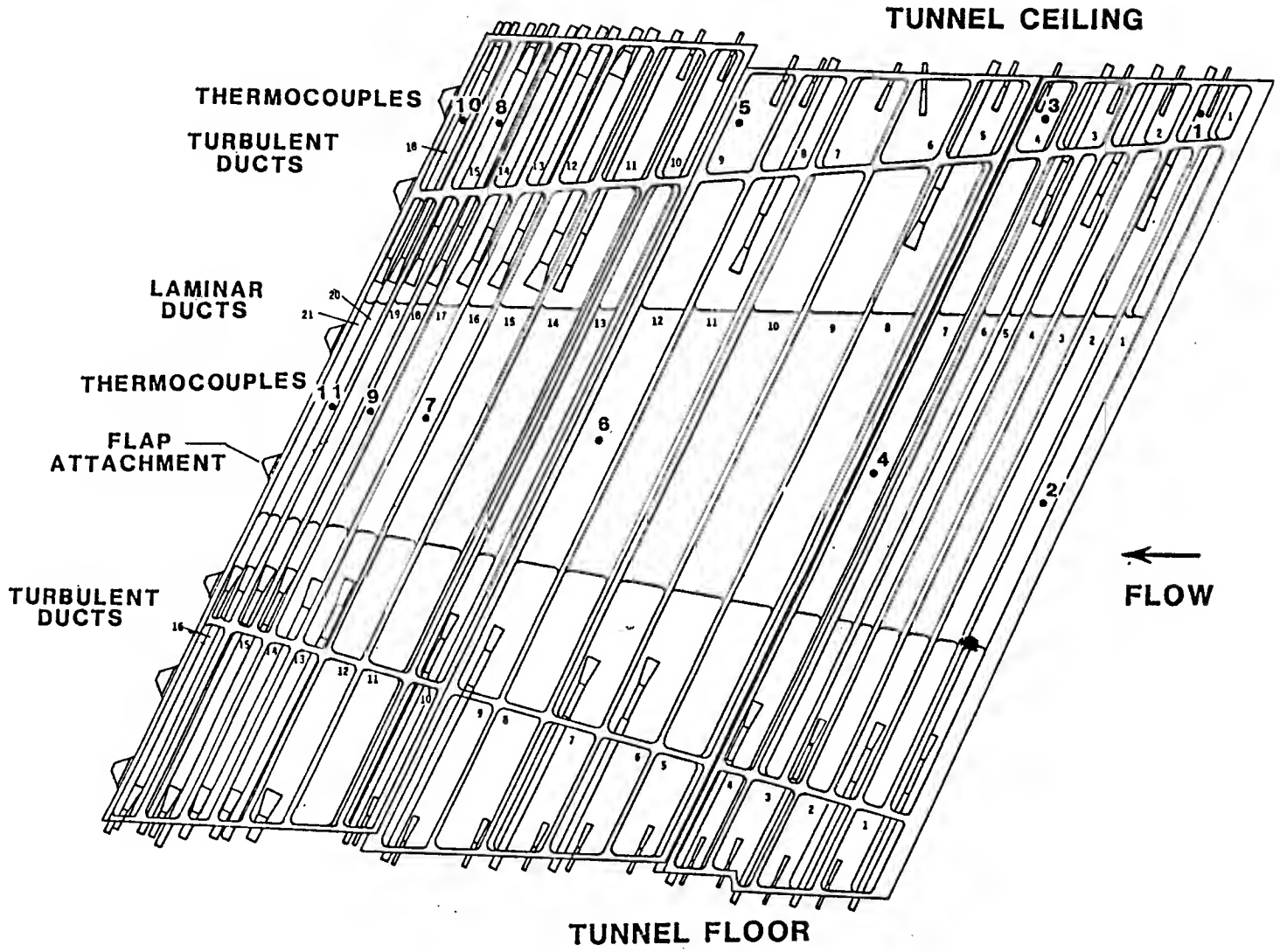

Figure 36. Sketch of nozzle locations.

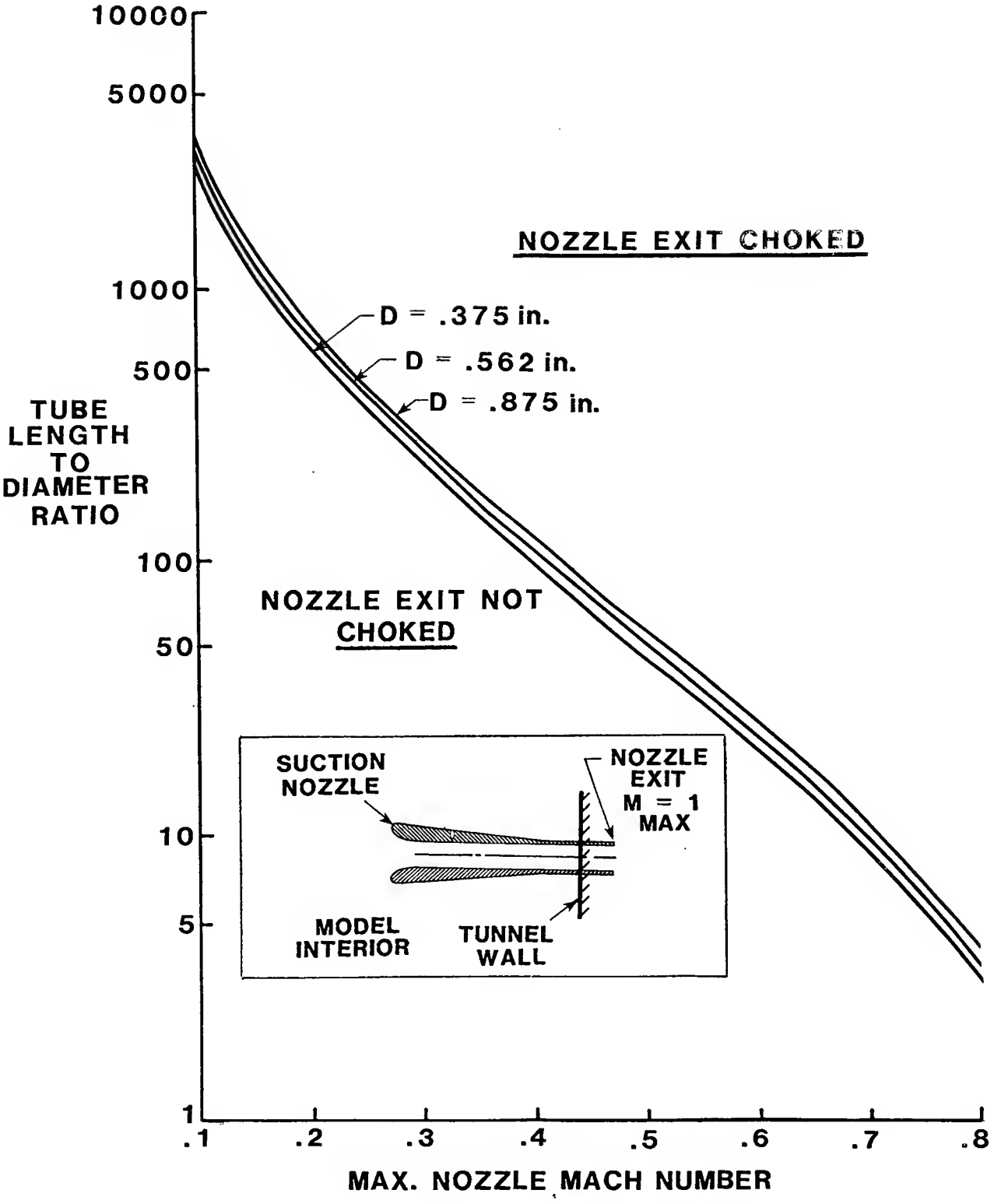

Figure 37. Length to diameter ratio requirements for non-choked suction flow.